

1 **Novel biomarkers for glycaemic deterioration in type 2 diabetes: an IMI**

2 **RHAPSODY study**

3 Roderick C Slieker, PhD^{1,2,*}, Louise A Donnelly, PhD^{3,*}, Livia Lopez-Noriega, PhD⁴,
4 Hermine Muniangi-Muhitu⁴, Elina Akalestou, PhD⁴, Mahsa Sheikh⁴, Eleni Georgiadou,
5 PhD⁴, Giuseppe N. Giordano, PhD⁵, Mikael Åkerlund, PhD⁵, Emma Ahlqvist, PhD⁵, Ashfaq
6 Ali, PhD⁶, Marko Barovic⁷, MSc, Gerard A Bouland, MSc², Frédéric Burdet, MSc⁸, Mickaël
7 Canouil, PhD⁹, Iulian Dragan, MSc⁸, Petra JM Elders, PhD¹⁰, Celine Fernandez, PhD⁵,
8 Andreas Festa, MD^{11,12}, Hugo Fitipaldi, MSc⁵, Phillippe Froguel^{9,13}, Valborg
9 Gudmundsdottir, PhD^{14,15}, Vilmundur Gudnason, MD, PhD^{14,15}, Mathias J. Gerl, PhD¹⁶,
10 Amber A van der Heijden, PhD¹⁰, Lori L Jennings, PhD¹⁷, Michael K. Hansen, PhD¹⁸, Min
11 Kim, PhD^{6,19}, Isabelle Leclerc MD PhD⁴, Christian Klose, PhD¹⁶, Dmitry Kuznetsov, PhD⁸,
12 Dina Mansour Aly, MSc⁵, Florence Mehl, PhD⁸, Diana Marek, PhD⁸, Prof Olle Melander,
13 PhD⁵, Anne Niknejad, MSc⁸, Filip Ottosson, MSc⁵, Imre Pavo, MD¹¹, Alexander Efanov,
14 PhD²⁰, Kevin Duffin²⁰, Timothy J. Pullen, PhD^{4,21}, Prof Kai Simons, PhD¹⁶, Prof. Michele
15 Solimena, PhD^{7,22}, Tommi Suviataival, PhD⁶, Asger Wretlind, MSc⁶, Prof Peter Rossing,
16 MD^{6,23}, Prof Valeriya Lyssenko, PhD^{24,25}, Cristina Legido Quigley, PhD^{6,19}, Prof Leif Groop,
17 PhD^{5,26}, Prof Bernard Thorens, PhD²⁷, Prof Paul W Franks, PhD^{5,28}, Mark Ibberson, PhD⁷,
18 Prof Joline WJ Beulens, PhD^{1,29}, Leen M 't Hart, PhD^{1,2,30,*}, †, Prof Ewan R Pearson, MD^{3,*},
19 ††, Prof Guy A Rutter, PhD^{*4,31,††}

20

21 ¹ Department of Epidemiology and Data Science, Amsterdam Public Health Institute,
22 Amsterdam Cardiovascular Sciences, Amsterdam UMC, location VUMC, Amsterdam, the
23 Netherlands

24 ² Department of Cell and Chemical Biology, Leiden University Medical Center, Leiden, the
25 Netherlands

26 ³ Population Health & Genomics, School of Medicine, University of Dundee, Dundee, UK.

27 ⁴ Section of Cell Biology and Functional Genomics, Division of Diabetes, Endocrinology and
28 Metabolism, Department of Metabolism, Digestion and Reproduction, Imperial College
29 London, London, U.K.

30 ⁵ Genetic and Molecular Epidemiology Unit, Lund University Diabetes Centre, Department
31 of Clinical Sciences, CRC, Lund University, SUS, Malmö, Sweden

32 ⁶ Steno Diabetes Center Copenhagen, Gentofte, Denmark

NOTE: This preprint reports new research that has not been certified by peer review and should not be used to guide clinical practice.

33 ⁷ Paul Langerhans Institute Dresden (PLID) of the Helmholtz Center Munich at the
34 University Hospital Carl Gustav Carus and Medical Faculty, Dresden, Germany.
35 ⁸ Vital-IT Group, SIB Swiss Institute of Bioinformatics, Lausanne, Switzerland
36 ⁹ INSERM U1283, CNRS UMR 8199, European Genomic Institute for Diabetes (EGID),
37 Institut Pasteur de Lille, University of Lille, Lille University Hospital, Lille, F-59000, France
38 ¹⁰ Department of General Practice and Elderly Care Medicine, Amsterdam Public Health
39 Research Institute, Amsterdam UMC–location VUmc, Amsterdam, the Netherlands
40 ¹¹ Eli Lilly Regional Operations GmbH, Vienna, Austria.
41 ¹² 1st Medical Department, LK Stockerau, Niederösterreich, Austria.
42 ¹³ Division of Systems Biology, Department of Diabetes, Endocrinology and Metabolism,
43 Imperial College London, London, UK
44 ¹⁴ Faculty of Medicine, University of Iceland, Reykjavik, Iceland
45 ¹⁵ Icelandic Heart Association, Kopavogur, Iceland
46 ¹⁶ Lipotype GmbH Dresden Germany
47 ¹⁷ Novartis Institutes for Biomedical Research, Cambridge, MA 02139, USA
48 ¹⁸ Cardiovascular and Metabolic Disease Research, Janssen Research & Development, Spring
49 House, Pennsylvania, U.S.A.
50 ¹⁹ Institute of Pharmaceutical Science, Faculty of Life Sciences and Medicines, King's
51 College London, London, United Kingdom
52 ²⁰ Lilly Research Laboratories, Eli Lilly and Company, Indianapolis, United States
53 ²¹ Department of Diabetes, Guy's Campus King's College London, U.K.
54 ²² Molecular Diabetology, University Hospital and Medical Faculty Carl Gustav Carus, TU
55 Dresden, Dresden, Germany.
56 ²³ Department of Clinical Medicine, University of Copenhagen, Copenhagen, Denmark
57 ²⁴ Department of Clinical Science, Center for Diabetes Research, University of Bergen,
58 Bergen, Norway
59 ²⁵ Genomics, Diabetes and Endocrinology Unit, Department of Clinical Sciences Malmö,
60 Lund University Diabetes Centre, Skåne University Hospital, Malmö, Sweden
61 ²⁶ Finnish Institute of Molecular Medicine, Helsinki University, Helsinki, Finland
62 ²⁷ Center for Integrative Genomics, University of Lausanne, CH-1015, Lausanne,
63 Switzerland
64 ²⁸ Department of Nutrition, Harvard School of Public Health, Boston, MA, USA
65 ²⁹ Julius Center for Health Sciences and Primary Care, University Medical Center Utrecht,
66 Utrecht, the Netherlands

67 ³⁰ Department of Biomedical Data Sciences, Section Molecular Epidemiology, Leiden
68 University Medical Center, Leiden, the Netherlands

69 ³¹ Lee Kong Chian School of Medicine, Nanyang Technological University, Singapore

70

71 * Contributed equally

72

73 Corresponding authors

74 † Leen 't Hart, PhD

75 Einthovenweg 20

76 2333ZC Leiden

77 The Netherlands

78 Telephone: +31 71 5269796

79 E-mail: lmthart@lumc.nl

80

81 †† Prof Ewan Pearson, MD

82 Ninewells Hospital

83 Dundee

84 DD1 9SY

85 United Kingdom

86 Telephone: +44 1382 383387

87 E-mail: E.Z.Pearson@dundee.ac.uk

88

89 ††† Prof Guy A Rutter, PhD

90 Section of Cell Biology and Functional Genomics,

91 Division of Diabetes, Endocrinology and Metabolism, Department of Metabolism, Digestion
92 and Reproduction,

93 Imperial College London,

94 Hammersmith Hospital Campus

95 Du Cane Road, London, W12 0NN, U.K

96 **ABSTRACT**

97 We have deployed a multi-omics approach in large cohorts of patients with existing type 2
98 diabetes to identify biomarkers for disease progression across three molecular classes,
99 metabolites, lipids and proteins. A Cox regression analysis for association with time to insulin
100 requirement in 2,973 patients in the DCS, ANDIS and GoDARTS cohorts identified
101 homocitrulline, isoleucine and 2-aminoadipic acid, as well as the bile acids glycocholic and
102 taurocholic acids, as predictive of more rapid deterioration. Increased levels of eight
103 triacylglycerol species, and lowered levels of the sphingomyelin SM 42:2;2 were also
104 predictive of disease progression. Of ~1,300 proteins examined in two cohorts, levels of GDF-
105 15/MIC1, IL-18RA, CRELD1, NogoR, FAS, and ENPP7 were associated with faster
106 progression, whilst SMAC/DIABLO, COTL1, SPOCK1 and HEMK2 predicted lower
107 progression rates. Strikingly, identified proteins and lipids were also associated with diabetes
108 incidence and prevalence in external replication cohorts. Implicating roles in disease
109 compensation, NogoR/RTN4R improved glucose tolerance in high fat-fed mice and tended to
110 improved insulin signalling in liver cells whilst IL-18R antagonised inflammatory IL-18
111 signalling towards nuclear factor kappa-B *in vitro*. Conversely, high NogoR levels led to islet
112 cell apoptosis. This comprehensive, multi-disciplinary approach thus identifies novel
113 biomarkers with potential prognostic utility, provides evidence for new disease mechanisms,
114 and identifies potential therapeutic avenues to slow diabetes progression.

115 INTRODUCTION

116 Type 2 diabetes is a progressive multifactorial disease which presently affects >400m
117 worldwide, with numbers expected to increase to > 700 m by 2045.¹ Biomarkers for the disease,
118 which provide a deeper understanding of the disease process, are therefore eagerly sought.
119 Importantly, their identification may improve prediction and personalized approaches to
120 disease treatment.²

121 Whilst many studies have examined associations between circulating biomarkers and
122 incident disease^{3,4}, to date few studies have explored changes associated with glycaemic
123 deterioration after the development of diabetes. Published studies (reviewed in ⁵) have
124 established that faster glycaemic deterioration is seen in those who are diagnosed younger, are
125 more obese at diagnosis, have lower HDL, and higher HbA1c. A few studies have investigated
126 genetic variants associated with more rapid progression with small and variable results⁵,
127 although a report on a Hong Kong Chinese population reported a replicated finding that a high
128 polygenic risk score consisting of 123 T2D risk variants was associated with increased
129 progression to insulin requirement.⁶ To date, no studies that have adopted a multi-omic
130 approach to biomarker discovery, or reported systematically how metabolites of different
131 classes impact on progression. Such associations have the potential to be clinically useful in
132 terms of prediction, as well as providing biological insights into the processes that drive
133 glycaemic deterioration in T2D.

134 In a collaboration based around the EU Innovative Medicines Initiative-2 Risk
135 Assessment and ProgreSsiOn of Diabetes (RHAPSODY) we have undertaken here to identify,
136 in three large European cohorts, biomarkers of diabetes progression of three molecular classes:
137 charged small molecules (metabolites), lipids and proteins. In this way, we identify novel
138 species and, in the case of two of the identified proteins, provide evidence through functional
139 studies in preclinical models for novel mechanisms of action in disease-relevant tissues.

140 **METHODS**

141

142 *Discovery cohorts*

143 Specific details on DCS⁷, GoDARTS⁸ and ANDIS⁹ have been described elsewhere.¹⁰ These
144 cohorts were selected based in part on satisfactory quality control for biomarkers stability in
145 stored samples.

146 Briefly, the Hoorn Diabetes Care System (DCS) cohort is a prospective cohort with
147 currently over 14,000 individuals with routine care data. The Ethical Review Committee of the
148 VU University Medical Center, Amsterdam approved the study. In 2008-2014, additional
149 blood sampling was done in 5,500 participants, who provided written informed consent. These
150 samples were used for this study. The turbidimetric inhibition immunoassay for haemolyzed
151 whole EDTA blood (Cobas c501, Roche Diagnostics, Mannheim, Germany) was used to
152 measure HbA1c. HDL (mmol/L) was measured enzymatically (Cobas c501, Roche
153 Diagnostics). C-peptide was measured on a DiaSorin Liaison (DiaSorin, Saluggia, Italy).

154 The Genetics of Diabetes Audit and Research Tayside Study (GoDARTS) is a cohort
155 of ~8,000 patients with T2D. The study was approved by the Tayside Medical Ethics
156 Committee and all individuals provided informed consent. Laboratory measurements were
157 measured in a non-fasted state. C-peptide was measured on a DiaSorin Liaison (DiaSorin,
158 Saluggia, Italy).

159 In the All New Diabetics in Scania (ANDIS) cohort, people with incident diabetes
160 within Scania County, Sweden were recruited from January 2008 until November 2016 and all
161 participants gave written informed consent. Regional ethics review committee in Lund
162 approved the study. An electro-chemiluminescence immunoassay was used to measure C-
163 peptide on a Cobas e411 (Roche Diagnostics, Mannheim, Germany) or a radioimmunoassay

164 (Human C-peptide RIA; Linco, St Charles, MO, USA; or Peninsula Laboratories, Belmont,
165 CA, USA). The Clinical Chemistry database was used to obtain HbA1c levels.

166

167 *Validation cohorts*

168 External validation was performed in four external cohorts, ACCELERATE, AGES-
169 Reykjavik, MDC-CC and DESIR. ACCELERATE is a clinical trial aimed at investigating the
170 effect of evacetrapib on major adverse cardiovascular outcomes and has been described
171 elsewhere.¹¹ For the current study we only included the 6,054 individuals in the untreated arm.
172 From this group, we selected 2,978 individuals with type 2 diabetes. In this group, 1003
173 individuals were excluded that did not have C-peptide levels or HbA1c levels, 72 were
174 excluded because the age at diagnosis was < 35 years, 31 were excluded because they were on
175 insulin at baseline and 22 were excluded because they had > 2 non-insulin glucose-lowering
176 drugs and HbA1c levels > 8.5%. The final set consisted of 1,850 individuals of which 162
177 reached the primary endpoint.

178 AGES-Reykjavik is a prospective population-based study from Iceland.^{12,13} In fasted
179 blood samples protein levels were measured with the Somalogic platform. At baseline there
180 were 4784 individuals free of diabetes and 654 with type 2 diabetes. Of 2,940 individuals free
181 of diabetes at baseline and with 5-year follow-up information, 112 developed type 2 diabetes.
182 ¹³ Identified proteins were tested against incident and prevalent type 2 diabetes using logistic
183 regression, adjusted for age and sex.

184 Malmö Diet and Cancer Cardiovascular Cohort (MDC-CC) is a population-
185 based cohort comprised of people living Malmö.¹⁴ Lipids were measured using the Lipotype
186 platform in 3,667 individuals of which 555 developed type 2 diabetes.¹⁵ Proteins were
187 measured using the Olink Proseek Multiplex proximity extension assay in 4915 individuals of

188 which 700 developed type 2 diabetes. Identified lipids and proteins were tested against incident
189 diabetes using Cox proportional hazard model adjusted for age, sex and BMI.

190 DESIR is a prospective population-based cohort comprised of middle-aged European
191 individuals. Metabolomics was measured by Metabolon (Durham, NC).¹⁶ Logistic regression
192 adjusted for age, sex and BMI was used to tested for an association between metabolites and
193 prevalent ($n = 43$) and incident ($n = 231$) type 2 diabetes versus controls ($n = 813$).

194

195 *Molecular measurements*

196 In the three discovery cohorts, those were selected with an age at diagnosis > 35 years, GAD
197 negative, GWAS data and with a blood sample within three years after diagnosis. The
198 metabolomics, lipidomics and proteomics groups were of different sizes (see further details
199 below). Individuals were ranked based on the time between diagnosis and sampling date and
200 those with the smallest time between diagnosis and sampling were selected. For metabolomics,
201 we selected 1,267 in DCS, 900 in GoDARTS and 900 in ANDIS. For lipidomics, 900
202 individuals were selected in DCS, GoDARTS and ANDIS. For proteomics, we selected 600
203 individuals in DCS and GoDARTS.

204

205 *Small charged molecule analytes*

206 In 2,973 individuals 19 small charged molecule analytes (referred to as metabolomics) using
207 UHLPC-MS/MS (UHLPLC: 1290 Infinity system from Agilent Technologies, Santa Clara,
208 CA, USA; MS/MS: 6460 triple quadrupole system from Agilent Technologies) relevant to
209 diabetes were quantified, which was used as the discovery set.¹⁷ In DCS, all samples passed
210 QC and were used in the analysis. In GoDARTS, three failed in QC and the remaining samples
211 were used for analysis. In ANDIS, 4 failed QC and of the 892 remaining samples, 811 were

212 free of the outcome at sampling. In addition, a validation set was generated comprised of 2,668
213 individuals (699 GoDARTS, 1,969 ANDIS).

214

215 *Lipid measurements*

216 Six hundred and fourteen (614) lipids were determined using a QExactive mass spectrometer
217 (Thermo Scientific) equipped with a TriVersa NanoMate ion source (Advion Biosciences) on
218 the Lipotype lipidomics platform (Lipotype, Dresden, Germany).¹⁸ Samples ($n = 2,608$) were
219 measured in batches of 84 samples each. Unprocessed mass spectra files were used to identify
220 lipids with LipotypeExplorer.¹⁹ Lipid identifications with a signal-to-noise ratio > 5 , and a signal
221 intensity 5-fold higher than in corresponding blank samples were considered for further data
222 analysis. Eight reference samples were used to apply batch correction and amounts were further
223 adjusted for analytical drift (p-value slope ≤ 0.05 and $R^2 \geq 0.75$ and the relative drift $> 5\%$).
224 Lipid nomenclature is used as described previously and SwissLipids database identifiers are
225 provided (**Table S1**).²⁰ After quality control 162 lipid species were used in this study. The
226 median coefficient of subspecies variation of the 162 lipids used as accessed by reference
227 samples was 9.49% across all three cohorts. In DCS, 900 individuals were included for
228 lipidomics measurements, all passed QC, and all were suitable for analysis. In GoDARTS, 898
229 individuals were included in the analysis, 1 failed QC and all 897 remaining samples were
230 included in the analysis. In ANDIS, 896 individuals were included in the analysis, 5 failed QC
231 and of the 891 remaining samples, 811 were free of the outcome at sampling.

232

233 *Protein measurements*

234 Proteins were measured on the SomaScan® Platform from Somalogic ($n = 1195$ proteins) on
235 the SomaLogic SOMAscan platform (Boulder, Colorado, USA) in 1,188 individuals. Top
236 associated proteins were validated in ANDIS ($n = 1992$) and ACCELERATE ($n = 1850$) using

237 ELISA with time to insulin requirement as the outcome. External validation was performed for
238 the top proteins based on P-value and/or effect size for which an ELISA was available or could
239 be developed.

240

241 *Primary endpoint*

242 The primary endpoint time to insulin requirement was defined as the period from diagnosis to
243 a clinical endpoint of the earlier of (i) starting sustained (more than 6 months duration) insulin
244 treatment or (ii) clinical requirement of insulin as indicated by two or more HbA1c
245 measurements >8.5% more than three months apart when on two or more non-insulin diabetes
246 therapies.²¹ In DCS, 600 individuals were included for proteomics measurements, 11 failed QC
247 and all were included for analysis. In GoDARTS, 600 individuals were included in the analysis,
248 1 failed QC and the 599 remaining samples were included in the analysis.

249

250 *Federated database*

251 All main analyses were performed on a federated database system. Opal, an open-source data
252 warehouse (Open Source Software for BioBanks, OBiBa) was used to store cohort data on
253 local nodes and remote analysis was performed in R using *DataSHIELD*²² and *dsSwissKnife* R
254 packages.²³ A central server was set up at the Swiss Institute of Bioinformatics to manage
255 federated node access, user administrator and software deployment. Local nodes were set up
256 at the respective cohorts. All data was harmonized according to the CDISC Study Data
257 Tabulation Model (www.cdisc.org) prior to inclusion into the federated database.

258

259 *Mendelian randomisation*

260 Genetic instruments for proteins, lipids and metabolites predictive of progression in the three
261 cohorts were obtained from published GWASs. Protein quantitative trait loci (QTLs) were

262 obtained from Gudmundsdottir et al.¹³ Lipid QTLs were obtained from Tabassum et al.²⁴
263 Metabolite QTLs were obtained from Lotta et al.²⁵ Only QTLs with P-values $< 5 \cdot 10^{-8}$ were
264 included. For traits with one instrument Wald ratio was used and for multiple instruments
265 inverse variance weighting. Instruments were excluded when in LD ($r^2 > 0.1$). Genetic
266 instruments for type 2 diabetes were obtained from the latest GWAS on incident type 2
267 diabetes.²⁶ Horizontal pleiotropy was estimated based on MR-Egger intercept. Cochran Q-
268 statistic was used to estimate heterogeneity of instruments.

269

270 *Cells and cell culture*

271 HEK-Blue IL-18 cells passages 1-16 (InvivoGen, USA) were cultured in 4.5 g/L glucose
272 Dulbecco's Modified Eagle's Medium (DMEM) supplemented with 10% foetal bovine serum
273 (FBS), 2 mM L-Glutamine, 50 U/ml penicillin, 50 µg/ml streptomycin (Sigma, UK) and 100
274 µg/ml Normocin (InvivoGen, USA). HEK-Blue IL-18 cells were designed to detect bioactive
275 IL-18 by monitoring the activation of the NF-κB and AP-1 pathways. They were generated by
276 stable transfection of HEK293 derived cells with the genes encoding IL-18R and IL-18
277 receptor accessory protein (IL-18RAP). Additionally, the TNF-α and the IL-1β responses have
278 been blocked to guarantee a specific respond to IL-18. Cells were seeded in T75 flasks and
279 sustained at 37°C in a humidified incubator containing 5% CO₂. Experiments were carried out
280 with HEK293 cells as well as a negative control.

281

282 *Cell transfection*

283 HEK-Blue IL-18 and HEK293 cells were seeded in 12-well plates at 30,000 per well and
284 transfected after 48 hours with both NF-κB and Renilla using Lipofectamine 2000 DNA
285 Transfection Reagent (Invitrogen, USA). For each well, 1.5 µl of Lipofectamine reagent was
286 diluted in 100µl Opti-MEM Gibco medium (Thermo Fisher, USA). The amount of 1 µl of NF-

287 κ B DNA at a concentration of 472.6 ng/ μ l and 1 μ l of Renilla at a concentration of 40 ng/ μ l
288 were also diluted in 100 μ l of Opti-MEM medium for each well, the diluted DNA mix was then
289 added to diluted Lipofectamine reagent and the transfection mix was incubated for 20 minutes
290 at RT. Cells were washed with 1ml of PBS and 400 μ l of Opti-MEM medium was added per
291 well. Cells were transfected with 200 μ l transfection mix each well. Medium was then changed
292 to complete growth medium (DMEM supplemented with 10% FBS, 2 mM L-Glutamine, 50
293 U/ml penicillin, 50 μ g/ml streptomycin and 100 μ g/ml Normocin) after 4 hours.

294

295 *Cell treatment and stimulation*

296 Transfected cells were stimulated with different concentrations of IL-18, IL-18R α or both to
297 measure changes in NF- κ B activation. Concentrations were made by diluting different volumes
298 of 1 μ M IL-18 and IL-18R α stock (diluted from freeze-dried powder in in distilled water) in
299 serum-free medium to exclude the effect of serum factors and cells were stimulated with 300
300 μ l of each condition per well of 12-well plate for 6 hours. Recombinant human IL-18 and rhIL-
301 18 R α /Fc chimera were obtained from MBL and R&D Systems respectively. Normal rabbit
302 IgG from Abcam (ab171870) was used as a negative control.

303

304 *Dual luciferase reporter assay*

305 Cells transfected with NF- κ B and stimulated with IL-18/IL-18R α were lysed following six
306 hours of treatment by adding 200 μ l of Promega Passive Lysis Buffer (PLB) to each well and
307 gentle shaking for 15 minutes at RT. Cell lysates were stored at -20°C and luciferase activity
308 was measured the next day using Promega Dual-Luciferase Reporter Assay System according
309 to manufacturer's instructions to study gene expression at the transcriptional level. Briefly,
310 Luciferase assay reagent II (LAR II) was dispensed into a luminometer tube for each condition.
311 Cell lysate was resuspended in tube containing LAR II and Firefly luciferase activity was

312 measured using Berthold Lumat LB 9507 Tube Luminometer. Next, Stop & Glo reagent was
313 added to each tube and the Renilla luciferase activities were measured. Measurements were
314 read with PuTTY software and all Firefly luciferase activities were normalized with Renilla
315 luciferase activities to obtain the NF- κ B signalling ratios using Microsoft Excel software.

316

317 *HepG2 cells stimulation and Western (immuno-) blotting*

318 HepG2 Cells (human hepatocytes) were cultivated in DMEM media with 1g/L of glucose,
319 supplemented with 10% SVF. HepG2 cells line were maintained at 37 °C and 5% CO₂. Cells
320 were treated with 0, 1nM, 10 nM, or 100 nM of NogoR (see above) or CRELD1 (Mouse Fc-
321 tagged, Sino Biological, Cat # 51149-M02H) recombinant proteins for 3 hours and then
322 stimulated with insulin for 15 minutes prior protein extraction. Cells were lysed in
323 radioimmunoprecipitation assay buffer (RIPA buffer: 20 mM Tris-HCl, 50 mM NaCl, 1 mM
324 Na₂-EDTA, 1 mM EGTA, 1% NP-40, 1% sodium deoxycholate) with 1% Phosphatase
325 Inhibitor Cocktails (P0044 and P5725, Sigma-Aldrich) and 1% Protease Inhibitor Cocktail
326 (P8340, Sigma-Aldrich). Protein concentration was measured using a Pierce BCA Protein
327 Assay Kit (Thermofisher, 23225) at 562 nm using a PHERAstar reader (BMG Labtech). After
328 protein transfer to a polyvinylidene Difluoride (PVDF) membrane (Millipore), membranes
329 were blocked with Tris-buffered saline 1X plus 0.1% (v/v) Tween (TBST), containing 4%
330 (w/v) BSA for 1h. Primary antibody incubation was performed overnight during rotation at 4
331 °C in TBST-4% (w/v) BSA and horseradish peroxidase (HRP)-conjugated secondary antibody
332 incubation was subsequently performed for 1 h in TBST-4% (w/v) milk powder. For
333 development we used Clarity Western ECL Substrate (Bio-Rad).

334

335

336

337 *In vivo metabolic tests*

338 All *in vivo* procedures were approved by the UK Home Office, according to the Animals
339 (Scientific Procedures) Act 1986 with local ethical committee (Imperial AWERB) approval
340 under personal project license (PPL) number PA03F7F07 to I.L. For the oral glucose tolerance
341 test (OGTT), C56BL6J mice (Charles River) maintained for four weeks on a high fat high
342 sucrose (HFHS) diet (a 58 kcal% Fat and Sucrose diet (D12331, Research Diet, New
343 Brunswick, NJ) were fasted for 16 h prior to experiment and received an oral glucose load (2
344 g/kg of body weight). For insulin tolerance tests, mice received an intraperitoneal injection of
345 insulin (1 IU/kg) after 3 h fasting. Blood glucose levels were determined by tail venepuncture
346 using a glucose meter (Accu-Chek; Roche, Burgess Hill, UK) at 0, 15, 30, 60 and 120 min.
347 after the glucose load. For insulin measurements blood was collected in EDTA covered tubes
348 at times 0, 15 and 30 min. after the glucose load (2 g/kg of body weight). Subsequently, blood
349 was centrifuged at 4000 x g for 20 min. at 4 °C and plasma was collected. Insulin was
350 determined by ELISA (CrystalChem, 90080), according to the manufacturer's instructions.
351 Daily intraperitoneal injections of NogoR were performed with indicated dose of NogoR
352 (mouse, His and Fc tag; Sino Biologicals Cat # 50106-M03H).

353

354 *Insulin secretion from mouse and human islets*

355 Mouse pancreatic islets were isolated from male C57BL/6 mice (Envigo, Indianapolis, IN) by
356 collagenase digestion. Use of animals was approved by Eli Lilly and Company's Institutional
357 Animal Care and Use Committee. Human pancreatic islets from listed cadaver organ donors
358 that were refused for pancreas or islet transplantation were obtained from Prodo Labs (Irvine,
359 CA) and InSphero AG (Schlieren, Switzerland) and were used in accordance with internal
360 review board ethical guidelines for use of human tissue. Islets were cultured in the complete
361 PIM(S) Prodo Islet Media (Prodo Labs) and RPMI 1640 medium (Invitrogen) supplemented

362 with 11 mm glucose, 10% (v/v) heat-inactivated foetal bovine serum (Invitrogen), 100 IU/ml
363 penicillin, and 100 µg/ml streptomycin (Invitrogen).

364 For insulin secretion in mouse islets, islets were incubated for 30 min. in Earle's
365 balanced salt solution (EBSS) buffer supplemented with 3 mM glucose and 0.1% BSA. Then
366 groups of three islets were selected and cultured with tested proteins at indicated glucose
367 concentration in 300 µL of EBSS for 60 minutes at 37°C. At the end of incubation, the
368 supernatant was collected and subjected to insulin analysis. To measure insulin secretion in
369 human pancreatic islets, single islets placed in a GravityTRAP 96-well plate (InSphero) were
370 washed and incubated for 30 minutes in 100 µL of EBSS supplemented with 0.1% BSA and 3
371 mM glucose. Then the buffer was replaced with 100 µL of EBSS containing indicated glucose
372 and protein concentrations and further cultured for 60 minutes at 37°C. At the end of
373 incubation, the supernatant was collected and submitted for insulin analysis. Insulin levels were
374 determined with the Meso Scale Discovery (Gaithersburg, MD) electrochemiluminescence
375 insulin assay.

376 For chronic incubation experiments, after overnight recovery human or mouse islets
377 were cultured in 12 well plate (20-30 islets per well) in the RPMI-1640 culture media
378 containing tested proteins for 72 h. At the end of incubation, islets were transferred into EBSS
379 supplemented with 3mM glucose and 0.1% BSA. Then, 1h insulin secretion in response to
380 elevated glucose in islets pre-treated with proteins was measured.

381

382 *Quantification of β -cell proliferation*

383 After overnight recovery, mouse or human islets were cultured for 72h in 12-well plates (200-
384 300 islets per well) in RPMI-1640 medium containing 5mM glucose, 2% FBS, 10 µM EdU
385 and tested proteins. At the end of incubation, islets were washed, dispersed into single cells
386 with the Accutase solution (Sigma) and placed in 96 well plate coated the Cell-Tak Cell and

387 Tissue Adhesive (Corning). Cells were fixed, permeabilized and stained with Click-iT Edu
388 HCS assay (ThermoFisher), PDX1 antibody (ab47308, Abcam) and Hoechst 33342
389 (ThermoFisher) nucleic acid dye. Cell images were captured and analysed using InSight
390 Imaging System (ThermoFisher).

391

392 *Islet cell apoptosis*

393 After 3-4 day culture, mouse or human islets were plated (1 islet per well) in the GravityTRAP
394 96-well plate (InSphero) in 100 μ l/well RPMI-1640 medium containing 11 mM glucose and
395 1% FBS. To induce cell death, islets were treated with glucose (25 mM) and palmitic acid (300
396 μ M palmitate conjugated with BSA), cytokine mixture (120 ng/ml TNF- α , 60 ng/ml IL-1B and
397 240 ng/ml IFN- γ , R&D Systems) or tunicamycin (0.03 μ g/ml, Tocris). After 72-hour
398 incubation, islets were caspase activity was measured with the Caspase-Glo 3/7 Assay
399 (Promega) according to manufacturer's protocol.

400

401 *Statistical analyses*

402 A Cox proportional hazard model was used to identify molecular risk factors for time to insulin
403 requirement in R (v3.6.0) remotely on each cohort federated node using the *dssCoxph* function
404 in *dsSwissKnife*. Three models with and without biomarkers were explored, where a primary
405 model was adjusted for age, sex and BMI. A second model was further adjusted for HDL and
406 C-peptide and the fully adjusted model additionally for diabetes duration and the use of glucose
407 lowering drugs. Models were stratified for HbA1c (strata: < 53 mmol/mol, 53-64 mmol/mol
408 and > 64 mmol/mol). Figures and meta-analysis was performed locally with R (v4.0.3).
409 Estimates in each cohort were meta-analysed using the *metagen* function from the R package
410 meta. P-values were adjusted for multiple testing using the Benjamini-Hochberg procedure and
411 a $P_{FDR} < 0.05$ was considered significant. Figures were made using ggplot2 (v3.3.2). Analysis

412 of cellular and metabolic data were performed using GraphPad Prism versions 7.0-9.0 (San
413 Diego, CA, U.S.A.) deploying ANOVA with appropriate post hoc correction for multiple
414 testing.

415 RESULTS

416

417 Cohort characteristics and modelling of glycaemic deterioration

418 Individuals from three cohorts, DCS, GoDARTS and ANDIS were included. In a subset
419 molecular characterization was performed of which characteristics are shown in **Table S2**. The
420 characteristics across the cohorts were comparable (**Table S2**). Male subjects were more
421 abundant in the cohorts (>55%), and the average age ranged from 61-67 years with a BMI of
422 30-32 kg/m². Glycated haemoglobin (HbA1c) levels were on average lowest in DCS
423 (median[Q25-Q75]: 47.08[42-50] mmol/mol), followed by GoDARTS (55.54[46-61]
424 mmol/mol) and ANDIS (60.06[46.0-68.0]). The time from diagnosis to sampling time ranged
425 from 0 to 2.63 years. Three phenotypic models were explored in the included cohorts which
426 showed concordance with BMI, use of glucose-lowering drugs being risk factors and age, HDL
427 and C-peptide being protective (**Table S3**).

428

429 Metabolites are associated with increased diabetes risk and progression

430 Out of the 19 small metabolites examined, five were associated with disease progression with
431 nominal significance in the base model (age, sex, BMI adjusted, P<0.05) in the meta-analysis
432 of three cohorts. These were homocitrulline (Hcit), aminoadipic acid (AADA), isoleucine (Ile),
433 glycocholic acid (GCA), taurocholic acid (TCA). Out of the five, the association of two
434 remained significant after multiple testing adjustment, including aminoadipic acid (AADA,
435 HR[CI]=1.11[1.04-1.19], P_{FDR} = 0.03) and homocitrulline (Hcit, 1.12[1.04-1.21], P_{FDR} = 0.04,
436 **Fig. 1, Table S4**). Both metabolites showed associations in the same direction in the replication
437 cohorts, but non-significant with attenuated effect sizes (AADA, HR[CI]=1.03[0.96-1.11];
438 Hcit 1.03[0.88-1.21]). In external validation cohorts, Hcit showed a trend as a risk factor for
439 incident diabetes (HR[CI] = 1.05[0.74-1.48]) in MDC. Based on a logistic model in DESIR,

440 Hcit was a risk factor for prevalent diabetes (OR[CI] = 1.32[1.05-1.66]), but not incident
441 diabetes (HR[CI] = 0.97[0.73-1.30]). AADA has previously been associated with a higher risk
442 of incident type 2 diabetes in Wang et al. (OR[CI] = 1.60[1.19-2.16]).²⁷ Finally, the most
443 consistent risk factor for time to insulin was isoleucine level, which was nominally significant
444 in the discovery cohort (HR[CI] = 1.09[1.00-1.20]), a risk factor for incident diabetes in MDC
445 (HR[CI] = 1.48[1.26-1.74]) and DESIR (OR[CI] = 23.88[3.13-182.31]) as well as prevalent
446 diabetes (OR[CI] = 10.94[3.94,30.32]). Finally, GCA and TCA were modest risk factors for
447 time to insulin requirement, with hazard ratios of 1.09[1.01-1.17] and 1.06[1.01-1.12],
448 respectively. In the replication set both TCA and GCA were in the same direction, but no longer
449 significant with hazard ratios of 1.09[0.91-1.31] and 1.04[0.94,1.12].

450

451 **Plasma triglyceride levels are markers of diabetes progression and incident diabetes**

452 Among the 162 lipids investigated, the levels of nine reached significance in the base model.
453 Among these eight lipids were a risk factor for early insulin requirement, and these were all
454 triglycerides (**Fig. 2, Table S5**). These eight lipids were also a risk factor for incident diabetes
455 in MDC (**Fig. 2**). A single lipid was *protective* for early insulin initiation (SM 42:2;2, HR[CI]
456 = 0.85[0.77-0.94]). Interestingly, SM 42:2;2 was a *risk factor* for incident diabetes in MDC
457 (HR[CI] = 1.16[1.06-1.27]). Further adjustment in the discovery cohort did attenuate the effect
458 size but the direction remained the same and four and three remained significant in the partly
459 and fully adjusted model, respectively (**Table S5**).

460

461 **Plasma proteins levels associate with diabetes progression and prevalent and incident** 462 **diabetes**

463 In the 1195 investigated plasma proteins, the levels of 98 were nominally associated with time
464 to insulin in the base model. Additional adjustment attenuated the hazard ratios only minimally

465 in both the partly and fully adjusted model. MIC-1/GDF15 was the protein associated with the
466 highest risk of progression (HR[CI] = 1.34[1.17-1.54]) and this association was replicated in
467 ACCELERATE (HR[CI] = 1.22[1.04-1.42]). The protein associated with the second highest
468 risk of progression was the Nogo receptor (NogoR, HR[CI] = 1.33[1.03-1.72], **Fig. 3, Table**
469 **S6**). In ANDIS, NogoR also replicated (HR[CI] = 1.20[1.07-1.34], **Fig. 3**). NogoR was also a
470 risk factor for incident (OR[CI] = 1.45[1.15-1.83]) and prevalent diabetes in AGES-Reykjavik
471 (OR[CI] = 1.77[1.60-1.95]). In the top associated proteins, four were protective including
472 SMAC, coactosin-like protein, testican-1 and HEMK2, of which HEMK2 was the most
473 protective (HR[CI] = 0.78[0.68-0.89]). In the AGES-Reykjavik study, HEMK2 was also
474 protective for prevalent diabetes (OR[CI] = 0.78[0.72,0.85]).

475

476

477 **Evidence of causality of biomarkers on incident diabetes based on Mendelian**

478 **Randomisation**

479 To assess causality of the identified biomarkers we would ideally have tested against the
480 genetics of time to insulin requirement in people with diabetes, but in the current study the
481 outcome was underpowered ($n = 14000$) and there is no publicly available data for time to
482 insulin genetic variants. Instead, we investigated the causality of biomarkers on type 2 diabetes.
483 We found no significant associations with incident diabetes for any of the top metabolites
484 (**Table 1**). However one of the nominally significant phosphatidyl ethanalamines, PE 18:0;0-
485 18:2;0 has support for a causal association with type 2 diabetes (**Table 1**, β [95%CI] = -0.07[-
486 0.12 – -0.02], $P = 3.89 \cdot 10^{-3}$). For the proteins, modest evidence of a causal relation was
487 observed for three proteins, GDF15 (β [95%CI] = 0.03[0.01– 0.05], $P = 2.68 \cdot 10^{-3}$), IL-18Ra
488 (β [95%CI] = 0.02[0.003– 0.03], $P = 0.014$) and FAS (β [95%CI] = 0.05[0.005-0.09], $P = 0.03$).
489 For the other protein biomarkers there was no evidence of a causal relation.

490

491 **Functional analyses of identified protein biomarkers**

492 *Glucose-stimulated insulin secretion.* We chose to study six protein biomarkers with greatest
493 effect size (GDF15, IL-18Ra, NogoR, CRELD1, FAS, ENPP7) and which accelerated
494 progression, *i.e.*, those which may plausibly exert a deleterious effect on insulin secretion or
495 action. None of these affected basal (3 mM glucose) or high (17 mM) glucose-stimulated
496 insulin secretion (GSIS) acutely (1h) or after longer incubations (48h) from either mouse (**Fig.**
497 **4a,b**) or human (**Fig. 4c**) islets. Glucagon-like peptide-1 (GLP-1) was used as a positive
498 control, and stimulated secretion at the higher glucose concentration, as expected.

499 To determine whether any of the examined protein biomarkers might affect pancreatic
500 beta cell mass, we next assessed their impact on beta cell apoptosis (**Fig. 5a-c**) and on
501 proliferation (d) in mouse islets. Of those examined, only IL-18Ra (3-fold), and NogoR (> 15-
502 fold) exerted an effect, increasing apoptosis in mouse islets. Dose response analyses (**Fig. 5b**)
503 revealed that the effects of NogoR were apparent only at high concentrations (> 1 nM) likely
504 to be above the normal physiological range. At 100 nM NogoR, but not IL-18Ra also enhanced
505 apoptosis in human islets (**Fig. 5c**). None of the tested compounds affected human islet
506 proliferation (**Fig. 5d**)

507

508 **NogoR improves glucose tolerance in vivo**

509 GDF15/MIC has been the subject of several earlier studies (see Discussion) and so was not
510 pursued further here. Since NogoR was the biomarker with the next-largest correlation with
511 disease progression, we next sought to determine whether this protein may influence glucose
512 homeostasis in vivo. Administered daily for two weeks to mice previously maintained on a
513 HFHS diet (four weeks²⁸), we observed a clear improvement in glucose tolerance in vivo versus
514 vehicle-injected animals (**Fig. 6a-d**). These changes were observed with no change in insulin
515 secretion (**Fig. 6e**).

516 Since these results suggested that NogoR might affect insulin signalling in disease
517 relevant tissues such as the liver, we measured the action of this protein on signalling events
518 downstream to insulin receptor activation, tested in HepG2 cells. Although not achieving
519 statistical significance, a trend was observed towards a potentiation of insulin-stimulated
520 phosphorylation of the protein kinase AKT on Ser473 after culture at different concentrations
521 of NogoR (1 nM, 10 nM and 100 nM) for 3h. (**SFig. 1a**). In contrast, no differences were
522 observed in insulin-stimulated Akt phosphorylation in HepG2 cells when cultured with
523 different concentrations of CRELD1 (**SFig. 1b**).

524

525 **Effect of IL-18Ra on IL-18Ra signalling**

526 After NogoR, IL-18Ra exerted the third strongest impact on diabetes progression (**Fig. 3**). We
527 therefore tested the effects of IL-18Ra in a reporter cell line expressing the IL-18R and a
528 luciferase construct under the control of the cytokine-regulated transcription factor, nuclear
529 factor κ B (NF- κ B; Methods). IL-18Ra attenuated the actions of IL-18 over a range of
530 concentrations at concentrations as low as 0.1 nM (**Fig. 7**).

531

532 **DISCUSSION**

533 We have undertaken a large multi-omic study, across three patient cohorts to discover novel
534 lipid, metabolite and protein biomarkers for diabetes progression. Many of our findings are
535 replicated in independent diabetes progression cohorts or validated for incident and/or
536 prevalent diabetes. In particular, we identify 9 lipids, 3 small charged molecules and 11 protein
537 biomarkers associated with accelerated glycaemic deterioration, and provide biological data in
538 pre-clinical models demonstrating possible mechanisms of action for NogoR and IL-18Ra.
539 Strikingly, measurements of proteins and lipid data reveal that the drivers of diabetes incidence
540 and prevalence may be similar to those of progression.

541

542 *Metabolites and glycaemic deterioration*

543 Two metabolites, Amino adipic Acid (AADA) and Homocitrulline (Hcit) were significantly
544 associated with diabetes progression, after correcting for multiple testing; three metabolites,
545 Isoleucine (Ile), and the bile acids GCA and TCA, were nominally associated with progression.
546 Isoleucine is a branched chain amino acid (BCAA) and a well-established risk factor for insulin
547 resistance and increased risk of type 2 diabetes.²⁹ Correspondingly, Ile was also associated with
548 both prevalent and incident diabetes in the current study. GCA and TCA are both existing
549 markers for pre-existing diabetes.³⁰

550 In previous studies, AADA was shown to be a risk factor for incident diabetes²⁷ and
551 Hcit with prevalent diabetes³¹, consistent with our findings. AADA is an alpha amino acid
552 formed as a downstream product of lysine oxidation by the action of myeloperoxidase
553 (MPO).³² Higher levels of plasma AADA have been associated with obesity, insulin resistance,
554 and increased risk of diabetes.^{27,33-35} Hcit levels have been associated with disrupted energy
555 metabolism in rat brains and have been linked to chronic renal failure.^{36,37} Of note, however,
556 where there was a sufficient genetic instrument, none of the metabolites we assessed with
557 mendelian randomisation were causally associated with diabetes risk, although it should be
558 noted that BCAAs have been suggested to be causal in the aetiology of type 2 diabetes.³⁸

559

560 *Lipids and glycaemic deterioration*

561 Nine lipids were associated with diabetes progression of which eight were associated with
562 increased risk which all belonged to the Triacylglycerol (TAG) class. In the external validation
563 data, all eight TAGs were associated with increased risk of type 2 diabetes. TAGs have
564 previously been associated with incident T2D risk.³⁹ TAG species levels also strongly decline
565 when obese individuals with diabetes undergo Roux-en-Y gastric bypass.⁴⁰ SM 42:2;2 was the

566 sole lipid associated with lower risk on progression towards to insulin, but was associated with
567 increased risk on future diabetes in the external validation data. A possible explanation for this
568 could be that metformin treatment influences the sphingomyelin levels including SM 42:2;2 as
569 has been shown in two studies in metformin treated HFD animals and human hepatocytes
570 respectively.^{41,42} The top associated lipids were also investigated for causality but generally
571 instruments were not available or no evidence was observed. The MR analysis of PE
572 18:0;0_18:2;0 supported a possible causal relation with incident diabetes. `

573

574 ***Proteins and glycaemic deterioration***

575 The protein with the strongest association with time to insulin was GDF-15/MIC1. This protein
576 has previously been implicated in diabetes incidence and the control of food intake^{43,44}, acting
577 via receptors in the hind brain.²⁸ GDF-15 has also been reported to serve as a useful biomarker
578 for impaired fasting glucose⁴⁵ and diabetic kidney disease⁴⁶ as well as a number of conditions
579 including cardiovascular disease^{47,48} GDF15 is strongly elevated following metformin
580 exposure, due to release from the gut.⁴⁹ Of note, we did not show any attenuation of the GDF15
581 signal with progression when adjusting for whether the patients were treated with metformin
582 at the time of blood sampling.

583 In addition, we identify several novel proteins biomarkers to be associated with
584 glycaemic deterioration in diabetes, including NogoR (RTN4), IL-18Ra, CRELD1, ENPP7 and
585 FAS. Interestingly, NogoR has previously been associated with prevalent diabetes and diabetes
586 incidence.¹³ In an effort to understand the potential impact of an increase in circulating NogoR
587 on glucose metabolism, we demonstrated that injection of this biomarker improves glucose
588 tolerance in high fat- high sucrose-fed mice, an effect likely to reflect improved insulin
589 sensitivity; insulin secretion was not significantly affected (indeed tended to be *increased* after
590 treatment). NogoR, (encoded by the *RTN4R* gene), is chiefly expressed in the central nervous

591 exist and mediates interactions between the myelin sheath and neurons, and has been
592 implicated in Alzheimer's disease.⁵⁰ In this setting, NogoR interacts with Oligodendrocyte
593 myelin glycoprotein (OMGP) and Nogo-A, present on myelin cells, to inhibit neuronal
594 regeneration.⁵¹ Thus NogoR serves as a receptor for Nogo-A but conceivably also the shorter
595 homologues Nogo-B and Nogo-C.⁵² Importantly in the context of systemic glucose
596 homeostasis, Nogo-B interacts with the Nogo-B receptor (NGBR, encoded by *NUS1*) and
597 knockout of *Nus1* in mice causes hepatic steatosis, possibly by interfering with insulin
598 signalling.⁵³ Furthermore, variants in the human *NUS1* gene including rs4443534 are
599 associated with altered type 2 diabetes risk.⁵⁴ Thus, by titrating Nogo-B (or other Nogo family
600 members) circulating NogoR may act indirectly on the liver to affect glucose storage or
601 glycogen breakdown. On the other hand, NogoR also enhanced cell death in pancreatic islets,
602 at least at high concentrations of this biomarker. The mechanisms involved in this action are
603 unclear given the absence of expression of the parental receptors of the interactors Nogo-A and
604 OMGP in islets.⁵⁵ Furthermore, the physiological relevance of these changes is uncertain since
605 concentrations at which NogoR exerted these effects *in vitro* (≥ 3 nM) comfortably exceeded
606 those which improved glucose metabolism *in vivo* (~ 0.7 nM). We suspect, therefore, that
607 positive effects of NogoR to improve insulin sensitivity may be predominant in most
608 physiological settings, though we do not exclude a shift towards deleterious actions on the
609 pancreas in disease settings.

610 CRELD1 (Cysteine-Rich with EGF-Like Domains 1, AVSD2, Cirrin) is a membrane-
611 bound Ca^{2+} -binding member of the EGF family critically required for normal development of
612 the heart⁵⁶ whose expression was recently shown to influence T-cell activity and immune
613 homeostasis.⁵⁷ Although we were not able to test the effects of this agent on glucose
614 homeostasis *in vivo* due to the unavailability of the human protein, we do provide evidence
615 that CRELD1 may regulate insulin signalling *in vitro*.

616 A recent Mendelian randomisation study¹³ provided nominally significant support for
617 a causal association between IL-18Ra and T2D, which was repeated here. Consistent with a
618 role in glucose homeostasis, IL-18 deletion in the mouse leads to obesity and insulin
619 resistance.⁵⁸ Conversely, after weight loss following exercise/diet or bariatric surgery in man,
620 a significant reduction in IL-18 concentrations was observed.^{59,60} IL-18 secretion also increased
621 in response to inflammasome activation and pyroptosis.⁶¹ We confirmed earlier studies⁶² which
622 demonstrated that an IL-18Ra:Fc fusion fragment inhibits the pro-inflammatory action of IL-
623 18. However, and in distinction to these earlier studies, measuring interferon-gamma (IFN-
624 gamma) production from mononuclear cells, the actions of IL-18Ra did not depend upon the
625 additional presence of IL-18Rbeta. We also noted that the concentrations of IL-18Ra as low as
626 0.1 nM efficiently inhibited the actions of a considerable excess (100 nM) of IL-18 potentially
627 suggesting a non-competitive action (*i.e.*, binding to the IL-18R at a separate site on the cellular
628 receptor to IL-18). Unexpectedly, IL-18Ra also influenced beta cell apoptosis in vitro. The
629 mechanisms involved here are unclear, however, since IL-18Ra expression levels in the beta
630 cell are low.⁶³ Finally, we note that IL-18Ra, CRELD1 and coactosin-like protein are all
631 involved in immune regulation, and might thus influence the inflammatory changes known to
632 be involved in T2D.⁶⁴

633 ENPP7 (Ectonucleotide pyrophosphatase/phosphodiesterase-7) is strongly expressed in
634 the small intestine where it is involved in sphingomyelin hydrolysis and the absorption of
635 ceramide and phosphocholine.⁶⁵ These processes might therefore be influenced by changed
636 circulating levels of ENPP7. FAS (FAS cell surface death receptor; TNF superfamily receptor-
637 6) is involved in caspase 3 and 8 activation and cell death⁶⁶ and might thus influence cell
638 survival in critical metabolic tissues. HSP 90B (heat shock protein 90 alpha family class B
639 member 1), encoded by *HSP90AB1*, is a molecular chaperone and regulator of protein
640 folding.⁶⁷

641 Other identified proteins were associated with protection from glycaemic deterioration
642 of diabetes. SMAC/IAPP-binding mitochondrial protein, also called DIABLO, is a
643 mitochondrially-associated protein which migrates to the cytosol upon the activation of
644 apoptosis, facilitating this process by restricting the activity of apoptotic inhibitors.⁶⁸ Lowered
645 levels of this protein in the plasma thus seem likely to reflect diminished levels of cell death in
646 disease-relevant (or other) tissues. Coactosin-like protein, encoded by the *COTL1* gene and
647 also called Coactosin-like F-actin binding protein, and CLP, is enriched in haematopoietic cells
648 (BioGPS), and regulates leukotriene synthesis. Low levels may therefore reflect more limited
649 inflammation in individuals whose disease deteriorates quickly. Testican-1, also called
650 SPOCK1, SPARC, and Osteonectin is enriched in the brain. The function of SPOCK1, a Ca²⁺
651 binding proteoglycan, is currently unknown, though roles in neuronal development⁶⁹ adipocyte
652 differentiation⁷⁰ and as an extracellular matrix factor controlling epithelial to mesenchymal
653 transition⁷¹ have been suggested. Finally, HEMK2 (N6AMT1, PrmC) is a ubiquitously-
654 expressed DNA methyl transferase.⁷²

655 To investigate causal associations, we undertook MR analysis of six of our identified
656 protein biomarkers that were associated with diabetes progression. We repeated previous
657 findings that GDF15 is causally associated with diabetes progression¹³ and found a possible
658 causal association for IL-18Ra and FAS. These data suggest that these two proteins are likely
659 to be causally associated with diabetes progression. The lack of a causal association of NogoR
660 with diabetes risk does suggest that NogoR may similarly not be causally associated with
661 diabetes progression, however, our functional studies do suggest a causal mechanism linking
662 NogoR with abnormal glucose metabolism.

663 This study has several limitations. Between cohorts there was heterogeneity, and this
664 was in part due to the nature of the cohorts, for example the ACCELERATE cohort is a clinical
665 trial which is different in setup than the discovery studies. Nonetheless, the results of the study

666 were robust, for example a large number of biomarkers were also found to be associated with
667 prevalent and incident diabetes. A third limitation is that for some protein biomarkers ELISA
668 assays are currently unavailable to validate the signals obtained in the SomaLogic screen.
669 Finally, in the Mendelian Randomization analysis we could only investigate the causal
670 association with diabetes risk, and some of the genetic instruments were weak, so the absence
671 of causality in MR analysis does not mean that our findings with diabetes progression were
672 non-causal. Indeed, plausible evidence for causality was subsequently obtained in functional
673 studies in preclinical models for NogoR and IL-18Ra.

674

675 **CONCLUSION**

676 Our findings provide new mechanistic insights into the mechanisms that underlie glycaemic
677 deterioration once diabetes has developed. Importantly, we describe novel biomarkers of
678 different chemical classes, several of which have not previously been associated with the
679 incident or prevalent disease, suggestive of potentially distinct mechanisms driving the two
680 stages of glycaemic deterioration - towards diabetes onset and after diabetes onset. We provide
681 direct functional analyses implicating two of these (NogoR, IL-18Ra) as likely to contribute
682 directly to disease progression. By better understanding the biological drivers of glycaemic
683 deterioration in diabetes it may be possible to target therapies to these processes to prevent or
684 slow diabetes progression, rather than simply to lower HbA1c, potentially transforming
685 diabetes treatments.

686

687 **ACKNOWLEDGEMENTS**

688 We acknowledge the support of the Health Informatics Centre, University of Dundee for
689 managing and supplying the anonymised data. The authors wish to thank the Core-IT group of
690 SIB Swiss Institute of Bioinformatics and in particular Jorge Molina for expert technical help

691 in setting up and maintaining the federated database. GR thanks Claudio Elgueta Karstegl for
692 technical support. The authors thank participants of the included cohorts.

693

694 **FUNDING**

695 ERP holds a Wellcome Trust New Investigator Award (102820/Z/13/Z). GAR was supported
696 by a Wellcome Trust Investigator Award (212625/Z/18/Z), MRC Programme grants
697 (MR/R022259/1, MR/J0003042/1, MR/L020149/1), an Experimental Challenge Grant (DIVA,
698 MR/L02036X/1), a Diabetes UK Project grant (BDA16/0005485). This project has received
699 funding from the Innovative Medicines Initiative 2 Joint Undertaking, under grant agreement
700 no. 115881 (RHAPSODY). This Joint Undertaking receives support from the European
701 Union's Horizon 2020 research and innovation programme and EFPIA. This work is supported
702 by the Swiss State Secretariat for Education, Research and Innovation (SERI), under contract
703 no. 16.0097. VaG is supported by the Icelandic Research Fund (grant no. 184845-051). The
704 Hoorn DCS cohort was supported by grants from the Netherlands Organisation for Health
705 Research and Development (113102006, 459001015)

706

707 **CONFLICTS OF INTEREST**

708 KS is CEO of Lipotype GmbH. KS and CK are shareholders of Lipotype GmbH. MJG is
709 employee of Lipotype GmbH. GAR has received grant funding and consultancy fees from Sun
710 Pharmaceuticals and Les Laboratoires Servier. MKH is an employee of Janssen Research &
711 Development, LLC. AF and IP are employees of Eli Lilly Regional Operations GmbH. The
712 AGES-Reykjavik proteomics study was supported by the Novartis Institute for Biomedical
713 Research, and protein measurements for the AGES-Reykjavik cohort were performed at
714 SomaLogic. L.L.J. is an employee and stockholder of Novartis. PR (Peter Rossing) has
715 received honoraria to Steno Diabetes Center Copenhagen for consultancy and teaching from

716 Astellas, Astra Zeneca, Boehringer Ingelheim, Bayer, Novo Nordisk, Sanofi, Gilead and Vifor
717 and research grants from Novo Nordisk and Astra Zeneca.

718

719 **AUTHOR CONTRIBUTION**

720 RCS, LAD, JWJB, LMTH, ERP, and GR designed the study. GR and RCS drafted the
721 manuscript. RCS, LAD, HF, GAB, MA performed the analyses. GR oversaw biomarker
722 shipments and assays, and coordinated all functional work in preclinical models. MS, MB,
723 LMtH, AAWAvH, PJME, JWJB, EA, LG, LAD, ERP provided patient samples for analysis.
724 LL, HM, EG, IL performed all studies on NogoR, EA, MS work on IL-18Ra. ID, DK, FB, DM,
725 AN, MI set up a federated node system for data-analysis. RCS, LAD, HF, DMA, EA, AA,
726 MJG, MK, FM, TS, AW, CLQ, MI were involved in the (clinical) data pre-processing and
727 quality control. GNG, AF, MKH, DMA, IP, TJP, BT, VL, LG, PWF, GAR contributed to the
728 data acquisition and project logistics. MJG, CK, KS generated the Lipotype data. CLQ, AA,
729 PR, AW, TS, FM generated the metabolomics data and/or were involved in the quality control.
730 FO, CF and OM acquired the MDC-CC data and performed the lipid and protein validation in
731 the MDC-CC. MC and PF performed the metabolite validation in DESIR. VaG, ViG and LLJ
732 performed the protein validation in the AGES-Reykjavik cohort. PJME and AAWAvH
733 acquired the data from the Hoorn DCS cohort. All authors contributed to the data interpretation.
734 All authors critically revised the manuscript and approved the final version. RCS and LAD are
735 the guarantors of the work.

736

737 **DATA DEPOSITION**

738 Summary statistics of lipidomic, proteomic and metabolomic data will be available from an
739 interactive Shiny dashboard available upon publication.

740

741 REFERENCES

- 742 1 International Diabetes Federation. Diabetes facts & figures. (2019).
743 2 Chung, W. K. *et al.* Precision Medicine in Diabetes: A Consensus Report From the
744 American Diabetes Association (ADA) and the European Association for the Study of
745 Diabetes (EASD). *Diabetes Care* **43**, 1617-1635, doi:10.2337/dci20-0022 (2020).
746 3 Ahluwalia, T. S., Kilpeläinen, T. O., Singh, S. & Rossing, P. Editorial: Novel
747 Biomarkers for Type 2 Diabetes. *Front Endocrinol (Lausanne)* **10**, 649,
748 doi:10.3389/fendo.2019.00649 (2019).
749 4 Kolberg, J. A. *et al.* Development of a type 2 diabetes risk model from a panel of
750 serum biomarkers from the Inter99 cohort. *Diabetes Care* **32**, 1207-1212, doi:10.2337/dc08-
751 1935 (2009).
752 5 Thakarakkattil Narayanan Nair, A. *et al.* The impact of phenotype, ethnicity and
753 genotype on progression of type 2 diabetes mellitus. *Endocrinol Diabetes Metab* **3**, e00108,
754 doi:10.1002/edm2.108 (2020).
755 6 Jiang, G. *et al.* Obesity, clinical, and genetic predictors for glycemic progression in
756 Chinese patients with type 2 diabetes: A cohort study using the Hong Kong Diabetes Register
757 and Hong Kong Diabetes Biobank. *PLoS Med* **17**, e1003209,
758 doi:10.1371/journal.pmed.1003209 (2020).
759 7 van der Heijden, A. A. *et al.* The Hoorn Diabetes Care System (DCS) cohort. A
760 prospective cohort of persons with type 2 diabetes treated in primary care in the Netherlands.
761 *BMJ open* **7**, e015599 (2017).
762 8 Hebert, H. L. *et al.* Cohort Profile: Genetics of Diabetes Audit and Research in
763 Tayside Scotland (GoDARTS). *Int J Epidemiol* **47**, 380-381j, doi:10.1093/ije/dyx140 (2018).
764 9 ANDIS - Alla Nya Diabetiker I Skåne, <<http://andis.ludc.med.lu.se/>> (2020).
765 10 Slieker, R. C. *et al.* Replication and cross-validation of T2D subtypes based on
766 clinical variables: an IMI-RHAPSODY study. *medRxiv*, doi:MEDRXIV/2020/248628
767 (2020).
768 11 Lincoff, A. M. *et al.* Evacetrapib and Cardiovascular Outcomes in High-Risk
769 Vascular Disease. *N Engl J Med* **376**, 1933-1942, doi:10.1056/NEJMoa1609581 (2017).
770 12 Harris, T. B. *et al.* Age, Gene/Environment Susceptibility-Reykjavik Study:
771 multidisciplinary applied phenomics. *Am J Epidemiol* **165**, 1076-1087,
772 doi:10.1093/aje/kwk115 (2007).
773 13 Gudmundsdottir, V. *et al.* Circulating Protein Signatures and Causal Candidates for
774 Type 2 Diabetes. *Diabetes* **69**, 1843-1853, doi:10.2337/db19-1070 (2020).
775 14 Ottosson, F. *et al.* A plasma lipid signature predicts incident coronary artery disease.
776 *Int J Cardiol*, doi:10.1016/j.ijcard.2021.01.059 (2021).
777 15 Fernandez, C. *et al.* Plasma Lipidome and Prediction of Type 2 Diabetes in the
778 Population-Based Malmö Diet and Cancer Cohort. *Diabetes Care* **43**, 366-373,
779 doi:10.2337/dc19-1199 (2020).
780 16 Yengo, L. *et al.* Impact of statistical models on the prediction of type 2 diabetes using
781 non-targeted metabolomics profiling. *Mol Metab* **5**, 918-925,
782 doi:10.1016/j.molmet.2016.08.011 (2016).
783 17 Ahonen, L. *et al.* Targeted Clinical Metabolite Profiling Platform for the Stratification
784 of Diabetic Patients. *Metabolites* **9**, doi:10.3390/metabo9090184 (2019).
785 18 Surma, M. A. *et al.* An automated shotgun lipidomics platform for high throughput,
786 comprehensive, and quantitative analysis of blood plasma intact lipids. *Eur J Lipid Sci*
787 *Technol* **117**, 1540-1549, doi:10.1002/ejlt.201500145 (2015).
788 19 Herzog, R. *et al.* LipidXplorer: a software for consensual cross-platform lipidomics.
789 *PLoS One* **7**, e29851, doi:10.1371/journal.pone.0029851 (2012).

- 790 20 Aimo, L. *et al.* The SwissLipids knowledgebase for lipid biology. *Bioinformatics* **31**,
791 2860-2866, doi:10.1093/bioinformatics/btv285 (2015).
- 792 21 Zhou, K. *et al.* Clinical and genetic determinants of progression of type 2 diabetes: a
793 DIRECT study. *Diabetes Care* **37**, 718-724, doi:10.2337/dc13-1995 (2014).
- 794 22 Wolfson, M. *et al.* DataSHIELD: resolving a conflict in contemporary bioscience--
795 performing a pooled analysis of individual-level data without sharing the data. *Int J*
796 *Epidemiol* **39**, 1372-1382, doi:10.1093/ije/dyq111 (2010).
- 797 23 Dragan, I., Sparsø, T., Kuznetsov, D., Slieker, R. & Ibberson, M. dsSwissKnife: An R
798 package for federated data analysis. *bioRxiv*, 2020.2011.2017.386813,
799 doi:10.1101/2020.11.17.386813 (2020).
- 800 24 Tabassum, R. *et al.* Genetic architecture of human plasma lipidome and its link to
801 cardiovascular disease. *Nat Commun* **10**, 4329, doi:10.1038/s41467-019-11954-8 (2019).
- 802 25 Lotta, L. A. *et al.* A cross-platform approach identifies genetic regulators of human
803 metabolism and health. *Nat Genet* **53**, 54-64, doi:10.1038/s41588-020-00751-5 (2021).
- 804 26 Mahajan, A. *et al.* Fine-mapping type 2 diabetes loci to single-variant resolution using
805 high-density imputation and islet-specific epigenome maps. *Nat Genet* **50**, 1505-1513,
806 doi:10.1038/s41588-018-0241-6 (2018).
- 807 27 Wang, T. J. *et al.* 2-Amino adipic acid is a biomarker for diabetes risk. *J Clin Invest*
808 **123**, 4309-4317, doi:10.1172/jci64801 (2013).
- 809 28 Tsai, V. W. *et al.* GDF15 mediates adiposity resistance through actions on GFRAL
810 neurons in the hindbrain AP/NTS. *Int J Obes (Lond)* **43**, 2370-2380, doi:10.1038/s41366-
811 019-0365-5 (2019).
- 812 29 Lynch, C. J. & Adams, S. H. Branched-chain amino acids in metabolic signalling and
813 insulin resistance. *Nat Rev Endocrinol* **10**, 723-736, doi:10.1038/nrendo.2014.171 (2014).
- 814 30 Andersen, E., Karlaganis, G. & Sjövall, J. Altered bile acid profiles in duodenal bile
815 and urine in diabetic subjects. *European journal of clinical investigation* **18**, 166-172 (1988).
- 816 31 Suhre, K. *et al.* Metabolic footprint of diabetes: a multiplatform metabolomics study
817 in an epidemiological setting. *PLoS One* **5**, e13953, doi:10.1371/journal.pone.0013953
818 (2010).
- 819 32 Lin, H. *et al.* Myeloperoxidase-mediated protein lysine oxidation generates 2-
820 amino adipic acid and lysine nitrile in vivo. *Free Radic Biol Med* **104**, 20-31,
821 doi:10.1016/j.freeradbiomed.2017.01.006 (2017).
- 822 33 Wijekoon, E. P., Skinner, C., Brosnan, M. E. & Brosnan, J. T. Amino acid
823 metabolism in the Zucker diabetic fatty rat: effects of insulin resistance and of type 2
824 diabetes. *Can J Physiol Pharmacol* **82**, 506-514, doi:10.1139/y04-067 (2004).
- 825 34 Gao, X. *et al.* Serum metabolic biomarkers distinguish metabolically healthy
826 peripherally obese from unhealthy centrally obese individuals. *Nutr Metab (Lond)* **13**, 33,
827 doi:10.1186/s12986-016-0095-9 (2016).
- 828 35 Cobb, J. *et al.* α -Hydroxybutyric Acid Is a Selective Metabolite Biomarker of
829 Impaired Glucose Tolerance. *Diabetes Care* **39**, 988-995, doi:10.2337/dc15-2752 (2016).
- 830 36 Viegas, C. M. *et al.* Experimental evidence that ornithine and homocitrulline disrupt
831 energy metabolism in brain of young rats. *Brain Res* **1291**, 102-112,
832 doi:10.1016/j.brainres.2009.07.021 (2009).
- 833 37 Desmons, A. *et al.* Homocitrulline: a new marker for differentiating acute from
834 chronic renal failure. *Clin Chem Lab Med* **54**, 73-79, doi:10.1515/cclm-2015-0398 (2016).
- 835 38 Lotta, L. A. *et al.* Genetic Predisposition to an Impaired Metabolism of the Branched-
836 Chain Amino Acids and Risk of Type 2 Diabetes: A Mendelian Randomisation Analysis.
837 *PLoS Med* **13**, e1002179, doi:10.1371/journal.pmed.1002179 (2016).
- 838 39 Rhee, E. P. *et al.* A genome-wide association study of the human metabolome in a
839 community-based cohort. *Cell Metab* **18**, 130-143, doi:10.1016/j.cmet.2013.06.013 (2013).

- 840 40 Graessler, J. *et al.* Lipidomic profiling before and after Roux-en-Y gastric bypass in
841 obese patients with diabetes. *Pharmacogenomics J* **14**, 201-207, doi:10.1038/tpj.2013.42
842 (2014).
- 843 41 Bornstein, S. *et al.* Metformin Affects Cortical Bone Mass and Marrow Adiposity in
844 Diet-Induced Obesity in Male Mice. *Endocrinology* **158**, 3369-3385, doi:10.1210/en.2017-
845 00299 (2017).
- 846 42 Wanninger, J. *et al.* Metformin reduces cellular lysophosphatidylcholine and thereby
847 may lower apolipoprotein B secretion in primary human hepatocytes. *Biochim Biophys Acta*
848 **1781**, 321-325, doi:10.1016/j.bbali.2008.04.012 (2008).
- 849 43 Mullican, S. E. *et al.* GFRAL is the receptor for GDF15 and the ligand promotes
850 weight loss in mice and nonhuman primates. *Nat Med* **23**, 1150-1157, doi:10.1038/nm.4392
851 (2017).
- 852 44 Patel, S. *et al.* GDF15 Provides an Endocrine Signal of Nutritional Stress in Mice and
853 Humans. *Cell Metab* **29**, 707-718.e708, doi:10.1016/j.cmet.2018.12.016 (2019).
- 854 45 Hong, J. H. *et al.* GDF15 Is a Novel Biomarker for Impaired Fasting Glucose.
855 *Diabetes Metab J* **38**, 472-479, doi:10.4093/dmj.2014.38.6.472 (2014).
- 856 46 Carlsson, A. C. *et al.* Growth differentiation factor 15 (GDF-15) is a potential
857 biomarker of both diabetic kidney disease and future cardiovascular events in cohorts of
858 individuals with type 2 diabetes: a proteomics approach. *Ups J Med Sci* **125**, 37-43,
859 doi:10.1080/03009734.2019.1696430 (2020).
- 860 47 Khan, S. & Rasool, S. T. Current use of cardiac biomarkers in various heart
861 conditions. *Endocr Metab Immune Disord Drug Targets*,
862 doi:10.2174/1871530320999200831171748 (2020).
- 863 48 Pang, L., Ge, L., Yang, P., He, H. & Zhang, H. Degradation of organophosphate
864 esters in sewage sludge: Effects of aerobic/anaerobic treatments and bacterial community
865 compositions. *Data Brief* **17**, 1030-1035, doi:10.1016/j.dib.2018.02.039 (2018).
- 866 49 Coll, A. P. *et al.* GDF15 mediates the effects of metformin on body weight and
867 energy balance. *Nature* **578**, 444-448, doi:10.1038/s41586-019-1911-y (2020).
- 868 50 Xu, Y. Q., Sun, Z. Q., Wang, Y. T., Xiao, F. & Chen, M. W. Function of Nogo-
869 A/Nogo-A receptor in Alzheimer's disease. *CNS Neurosci Ther* **21**, 479-485,
870 doi:10.1111/cns.12387 (2015).
- 871 51 Llorens, F., Gil, V. & del Río, J. A. Emerging functions of myelin-associated proteins
872 during development, neuronal plasticity, and neurodegeneration. *Faseb j* **25**, 463-475,
873 doi:10.1096/fj.10-162792 (2011).
- 874 52 Zhang, R., Tang, B. S. & Guo, J. F. Research advances on neurite outgrowth inhibitor
875 B receptor. *J Cell Mol Med* **24**, 7697-7705, doi:10.1111/jcmm.15391 (2020).
- 876 53 Hu, W. *et al.* Nogo-B receptor deficiency increases liver X receptor alpha nuclear
877 translocation and hepatic lipogenesis through an adenosine monophosphate-activated protein
878 kinase alpha-dependent pathway. *Hepatology* **64**, 1559-1576, doi:10.1002/hep.28747 (2016).
- 879 54 Type 2 diabetes Knowledge Portal.
880 <[https://t2d.hugeamp.org/region.html?chr=6&end=118081803&phenotype=HEIGHT&start=](https://t2d.hugeamp.org/region.html?chr=6&end=118081803&phenotype=HEIGHT&start=117946665)
881 [117946665](https://t2d.hugeamp.org/region.html?chr=6&end=118081803&phenotype=HEIGHT&start=117946665)> (2021).
- 882 55 Wu, C., Jin, X., Tsueng, G., Afrasiabi, C. & Su, A. I. BioGPS: building your own
883 mash-up of gene annotations and expression profiles. *Nucleic Acids Res* **44**, D313-316,
884 doi:10.1093/nar/gkv1104 (2016).
- 885 56 Rupp, P. A. *et al.* Identification, genomic organization and mRNA expression of
886 CRELD1, the founding member of a unique family of matricellular proteins. *Gene* **293**, 47-
887 57, doi:10.1016/s0378-1119(02)00696-0 (2002).
- 888 57 Bonaguro, L. *et al.* CRELD1 modulates homeostasis of the immune system in mice
889 and humans. *Nat Immunol* **21**, 1517-1527, doi:10.1038/s41590-020-00811-2 (2020).

- 890 58 Netea, M. G. *et al.* Deficiency of interleukin-18 in mice leads to hyperphagia, obesity
891 and insulin resistance. *Nat Med* **12**, 650-656, doi:10.1038/nm1415 (2006).
- 892 59 Esposito, K. *et al.* Effect of weight loss and lifestyle changes on vascular
893 inflammatory markers in obese women: a randomized trial. *Jama* **289**, 1799-1804,
894 doi:10.1001/jama.289.14.1799 (2003).
- 895 60 Botella-Carretero, J. I. *et al.* The decrease in serum IL-18 levels after bariatric surgery
896 in morbidly obese women is a time-dependent event. *Obes Surg* **17**, 1199-1208,
897 doi:10.1007/s11695-007-9202-3 (2007).
- 898 61 Pickering, R. J. & Bryant, C. E. Preventing pores and inflammation. *Science* **369**,
899 1564-1565, doi:10.1126/science.abe0917 (2020).
- 900 62 Reznikov, L. L. *et al.* The combination of soluble IL-18Ralpha and IL-18Rbeta chains
901 inhibits IL-18-induced IFN-gamma. *J Interferon Cytokine Res* **22**, 593-601,
902 doi:10.1089/10799900252982070 (2002).
- 903 63 Blodgett, D. M. *et al.* Novel Observations From Next-Generation RNA Sequencing of
904 Highly Purified Human Adult and Fetal Islet Cell Subsets. *Diabetes* **64**, 3172-3181,
905 doi:10.2337/db15-0039 (2015).
- 906 64 Jafaripour, S., Sedighi, S., Jokar, M. H., Aghaei, M. & Moradzadeh, M.
907 Inflammation, diet, and type 2 diabetes: a mini-review. *J Immunoassay Immunochem* **41**,
908 768-777, doi:10.1080/15321819.2020.1750423 (2020).
- 909 65 Duan, R. D. *et al.* Purification, localization, and expression of human intestinal
910 alkaline sphingomyelinase. *J Lipid Res* **44**, 1241-1250, doi:10.1194/jlr.M300037-JLR200
911 (2003).
- 912 66 Scott, F. L. *et al.* The Fas-FADD death domain complex structure unravels signalling
913 by receptor clustering. *Nature* **457**, 1019-1022, doi:10.1038/nature07606 (2009).
- 914 67 Chadli, A. *et al.* GCUNC-45 is a novel regulator for the progesterone receptor/hsp90
915 chaperoning pathway. *Mol Cell Biol* **26**, 1722-1730, doi:10.1128/mcb.26.5.1722-1730.2006
916 (2006).
- 917 68 Du, C., Fang, M., Li, Y., Li, L. & Wang, X. Smac, a mitochondrial protein that
918 promotes cytochrome c-dependent caspase activation by eliminating IAP inhibition. *Cell* **102**,
919 33-42, doi:10.1016/s0092-8674(00)00008-8 (2000).
- 920 69 Charbonnier, F., Périn, J. P., Roussel, G., Nussbaum, J. L. & Alliel, P. M. [Cloning of
921 testican/SPOCK in man and mouse. Neuromuscular expression perspectives in pathology]. *C*
922 *R Seances Soc Biol Fil* **191**, 127-133 (1997).
- 923 70 Alshargabi, R. *et al.* SPOCK1 induces adipose tissue maturation: New insights into
924 the function of SPOCK1 in metabolism. *Biochem Biophys Res Commun* **533**, 1076-1082,
925 doi:10.1016/j.bbrc.2020.09.129 (2020).
- 926 71 Sun, L. R., Li, S. Y., Guo, Q. S., Zhou, W. & Zhang, H. M. SPOCK1 Involvement in
927 Epithelial-to-Mesenchymal Transition: A New Target in Cancer Therapy? *Cancer Manag*
928 *Res* **12**, 3561-3569, doi:10.2147/cmar.S249754 (2020).
- 929 72 Figaro, S., Scrima, N., Buckingham, R. H. & Heurgué-Hamard, V. HemK2 protein,
930 encoded on human chromosome 21, methylates translation termination factor eRF1. *FEBS*
931 *Lett* **582**, 2352-2356, doi:10.1016/j.febslet.2008.05.045 (2008).
- 932

933 **TABLES**

934

935 *Table 1. Mendelian randomization analysis on metabolites, lipids and proteins against incident type 2*
 936 *diabetes*

Metabolites

| <i>variable</i> | <i>method</i> | <i>nsnp</i> | <i>Beta</i> | <i>Lower</i> | <i>Upper</i> | <i>P-value</i> | <i>Egger intercept</i> | <i>Q</i> | <i>Q(df)</i> | <i>Q(Pvalue)</i> |
|-----------------|---------------|-------------|-------------|--------------|--------------|----------------|------------------------|----------|--------------|------------------|
| AADA | IVW | 2 | 0.02 | -0.09 | 0.13 | 0.77 | | 0.02 | 1 | 0.88 |
| Citrulline | IVW | 6 | -0.01 | -0.29 | 0.28 | 0.97 | -0.04 | 83.02 | 5 | <0.001 |
| Isoleucine | IVW | 5 | -0.06 | -0.94 | 0.83 | 0.90 | -0.11 | 127.69 | 4 | <0.001 |
| Leucine | IVW | 6 | -0.08 | -0.74 | 0.58 | 0.81 | -0.07 | 127.77 | 5 | <0.001 |

Lipids

| <i>variable</i> | <i>method</i> | <i>nsnp</i> | <i>Beta</i> | <i>Lower</i> | <i>Upper</i> | <i>P-value</i> | <i>Egger intercept</i> | <i>Q</i> | <i>Q(df)</i> | <i>Q(Pvalue)</i> |
|------------------|---------------|-------------|-------------|--------------|--------------|-----------------------|------------------------|----------|--------------|------------------|
| PE 18:0;0_18:2;0 | IVW | 3 | -0.07 | -0.12 | -0.02 | 3.89·10 ⁻³ | 0.02 | 5.53 | 2 | 0.06 |
| SM 42:2;2 | IVW | 2 | 0.00 | -0.07 | 0.07 | 0.99 | | 0.91 | 1 | 0.34 |
| TAG 50:1;0 | IVW | 2 | 0.01 | -0.04 | 0.05 | 0.75 | | 0.00 | 1 | 0.97 |

Proteins

| <i>variable</i> | <i>method</i> | <i>nsnp</i> | <i>Beta</i> | <i>Lower</i> | <i>Upper</i> | <i>pval</i> | <i>Egger intercept</i> | <i>Q</i> | <i>Q(df)</i> | <i>Q(Pvalue)</i> |
|-----------------|---------------|-------------|-------------|--------------|--------------|-----------------------|------------------------|----------|--------------|------------------|
| GDF15 | IVW | 8 | 0.03 | 0.01 | 0.05 | 2.68·10 ⁻³ | 0.01 | 8.83 | 7 | 0.27 |
| IL-18Ra | IVW | 14 | 0.02 | 0.003 | 0.03 | 0.01 | 0.00 | 6.75 | 13 | 0.91 |
| FAS | IVW | 4 | 0.05 | 0.005 | 0.09 | 0.03 | 0.00 | 6.34 | 3 | 0.10 |
| RTN4R | IVW | 10 | -0.01 | -0.03 | 0.01 | 0.28 | -0.01 | 4.16 | 9 | 0.90 |
| ENPP7 | IVW | 4 | 0.01 | -0.01 | 0.02 | 0.34 | 0.00 | 0.85 | 3 | 0.84 |
| CRELD1 | IVW | 7 | 0.01 | -0.01 | 0.02 | 0.43 | 0.01 | 7.33 | 6 | 0.29 |

937 *IVW, inverse variance weighting; nsnp, number of instruments*

938 **FIGURE LEGENDS**

939 **Figure 1 Metabolites associated with diabetes development and progression. a)** Hazards
940 of a time to insulin model in the three discovery cohorts plus two replication sets in two of the
941 three cohorts and their respective meta-analyses (Model 1). The figure shows the five
942 nominally significant metabolites, with Hcit and AADA being also significant after multiple
943 testing. **b)** Hazards of incident diabetes in MDC based on a Cox proportional hazards model
944 adjusted for age, sex and BMI. **c)** Odds ratios of incident and prevalent diabetes in DESIR
945 based on a logistic regression model adjusted for age, sex and BMI.

946

947 **Figure 2. Lipids associated with diabetes development and progression. a)** Hazards of a
948 time to insulin model in the three discovery cohorts and the meta-analysed hazards (Model
949 1). The figure shows the nine significant lipids after multiple testing. **b)** Hazard models of
950 incident diabetes in MDC based on a Cox proportional hazards model.

951

952 **Figure 3. Proteins in plasma or serum associated with time to insulin requirement. a)**
953 Top proteins associated with time to insulin requirement. Shown is the top 10 based on P-
954 value plus Nogo receptor, which showed the largest risk of the top hundred proteins. X-axis,
955 hazard ratio on a log₂ scale and studies on the y-axis. **b)** Association between protein levels
956 and incident diabetes. X-axis, odds ratio on a log₂ scale. **c)** Association between protein
957 levels and prevalent diabetes. X-axis, odds ratio on a log₂ scale.

958

959 **Figure 4. Impact of identified biomarkers on insulin secretion from mouse (a,b) and**
960 **human (c) islets.** Incubations were performed for 30 min. at the indicated concentrations of
961 glucose, and secreted insulin measured using an electrochemiluminescence assay. ***, ** p =

962 0.001, 0.01 compared to vehicle; ## $p < 0.01$ vs 3 mM glucose. Comparisons by one-way
963 ANOVA in each case. Other details are given in the Methods Section.

964

965 **Figure 5** Impact of identified biomarkers on apoptosis (a-c) or proliferation (d) in mouse or
966 human islets as indicated. Test compounds were added at 100 nM unless otherwise indicated.
967 *,*** $p < 0.05$, 0.001 by one-way ANOVA for the effects of the indicated compounds *versus*
968 vehicle. See Methods for other details.

969

970 **Figure 6. NogoR enhances glucose clearance and insulin sensitivity in mice.** Two separate
971 cohorts of wild-type male C57BL/6J mice were maintained on a high fat diet for six weeks,
972 then injected for 14 consecutive days with saline or 100 ng (2.1 pmol/animal) recombinant
973 NogoR. **a,b**) Body weights of cohort one and circulating glucose levels during an oral glucose
974 tolerance test (OGTT; 2g/kg) pre-NogoR treatment $n = 5$. **c,d**) Body weights and blood glucose
975 levels after an oral glucose load (2g/kg) of cohort one after NogoR treatment. $n = 5$. **e**) Plasma
976 insulin levels after an oral glucose load (2g/kg) in cohort 1. $n = 5$ per group. **f, g**) Post-treatment
977 body weights of cohort 2 and circulating glucose levels after receiving an intraperitoneal
978 injection of 1 IU/kg of insulin. Data are represented as the mean \pm SEM. * p -value < 0.05
979 Student T-test.

980

981 **Figure 7. NF- κ B activation in HEK293 cells overexpressing IL-18R and co-stimulated**
982 **with IL-18 and IL-18R α .** IL-18R HEK cells stimulated for 6 h with 100, 50, 20, 10, 5, 2 and
983 1 nM of IL-18 alone, and also with 100, 10, 1 and 0.1nM of IL-18R α . IL-18 and IL-18R α
984 concentrations were tested in triplicate and NF- κ B activation was measured using dual
985 luciferase reporter assay. Curve fitting was done using non-linear regression with GraphPad

986 Prism 9.0.0 for log(agonist) vs. response (a) and inhibitor vs. response (b).

987

988 SUPPLEMENTARY FIGURE LEGENDS

989

990 **Supp Figure 1.** Effects of NogoR and of CRELD1 on insulin signalling in vitro. HepG2 cells
991 were cultured for 3 hours with 0, 1, 10 or 100 nM of NogoR (a) or CRELD1 (b) and 100 nM
992 of insulin for 15 minutes prior protein extraction. a) Protein AKT and pSer473 AKT levels in
993 Hepg2 treated with different concentrations of NogoR ($n = 3$). b) Protein AKT and pSer473
994 AKT levels in HepG2 treated with different concentrations of NogoR ($n = 3$). Data are
995 represented as the mean \pm SEM and were analysed by one-way ANOVA.

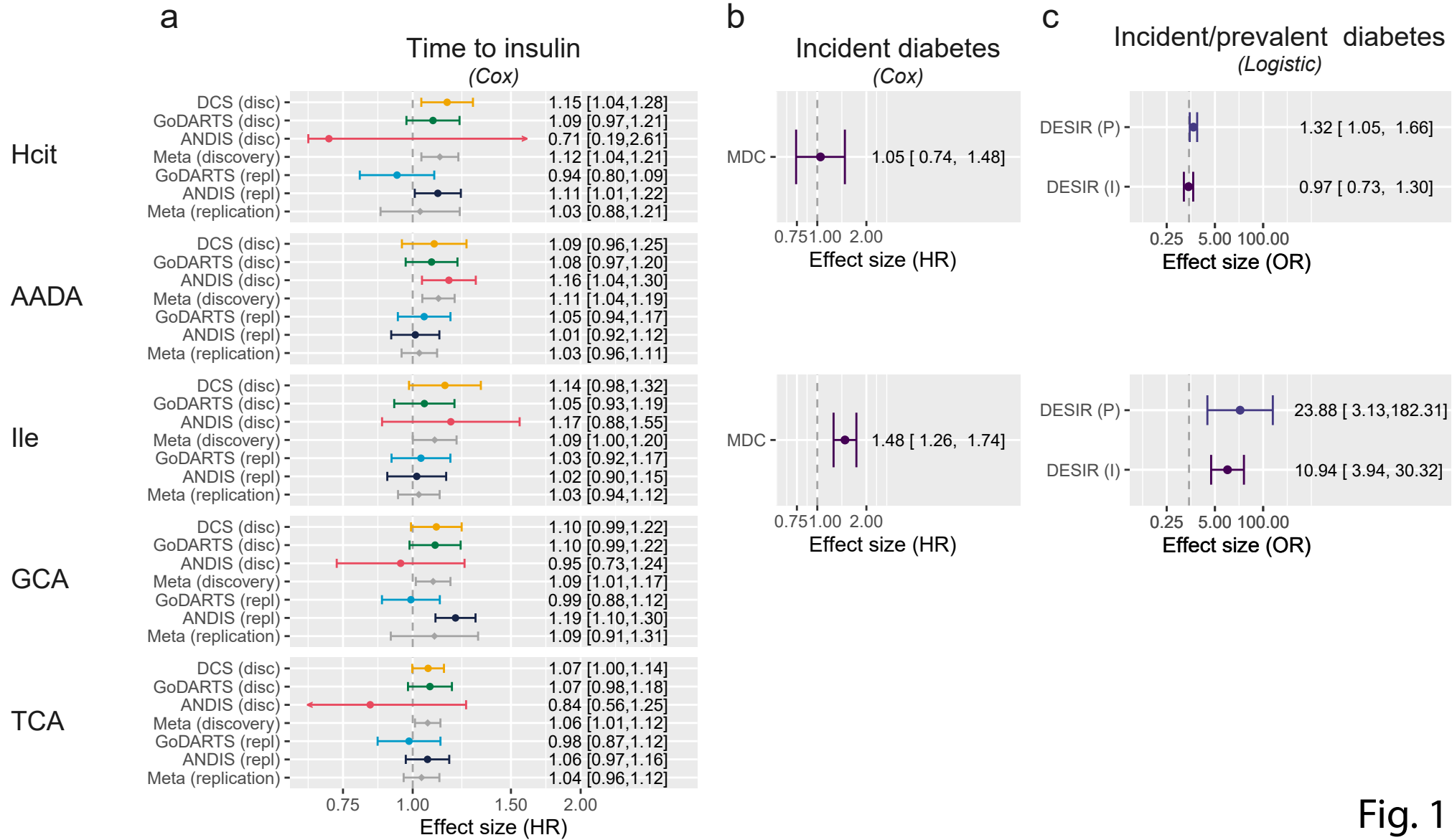


Fig. 1

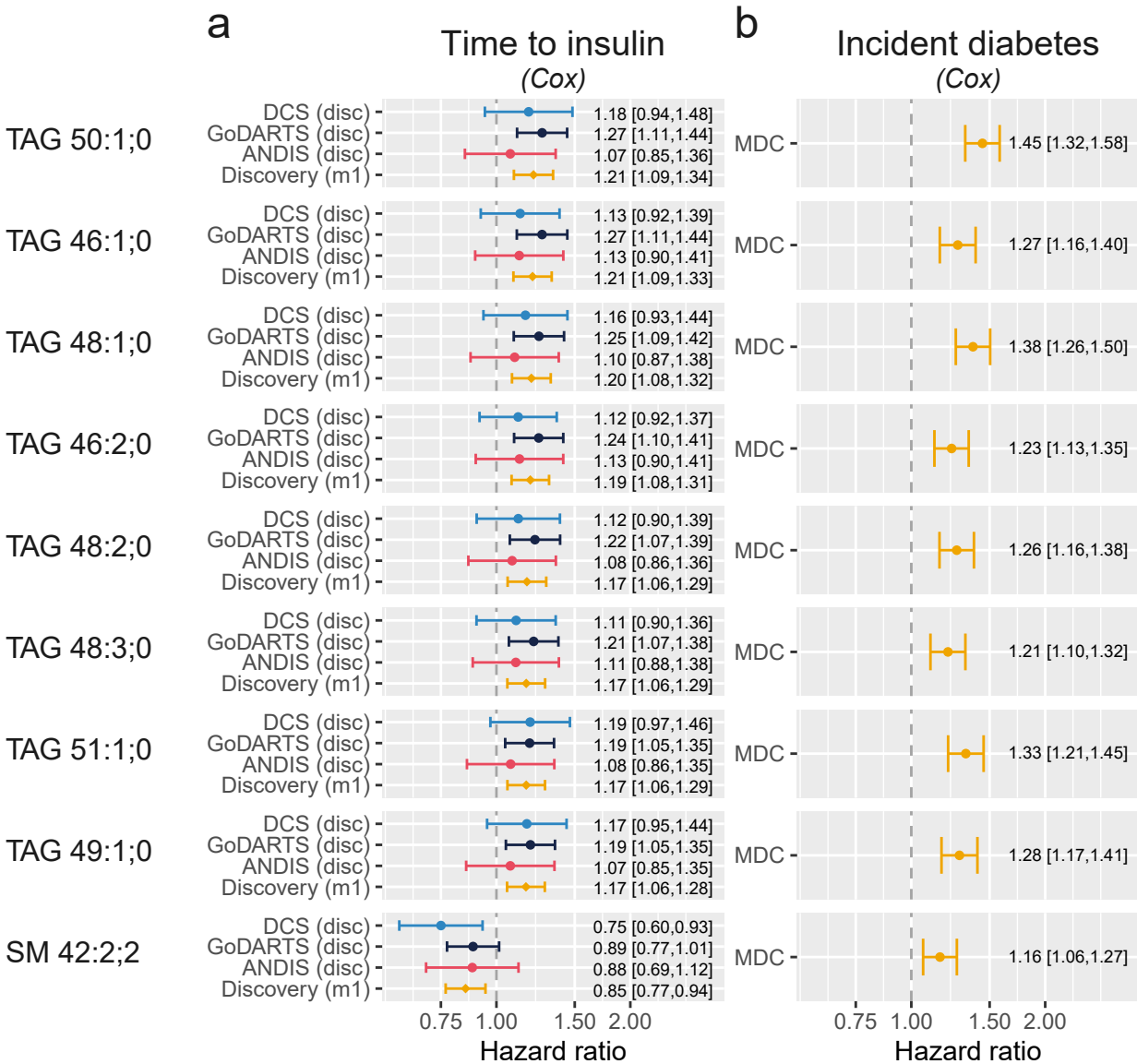


Fig. 2

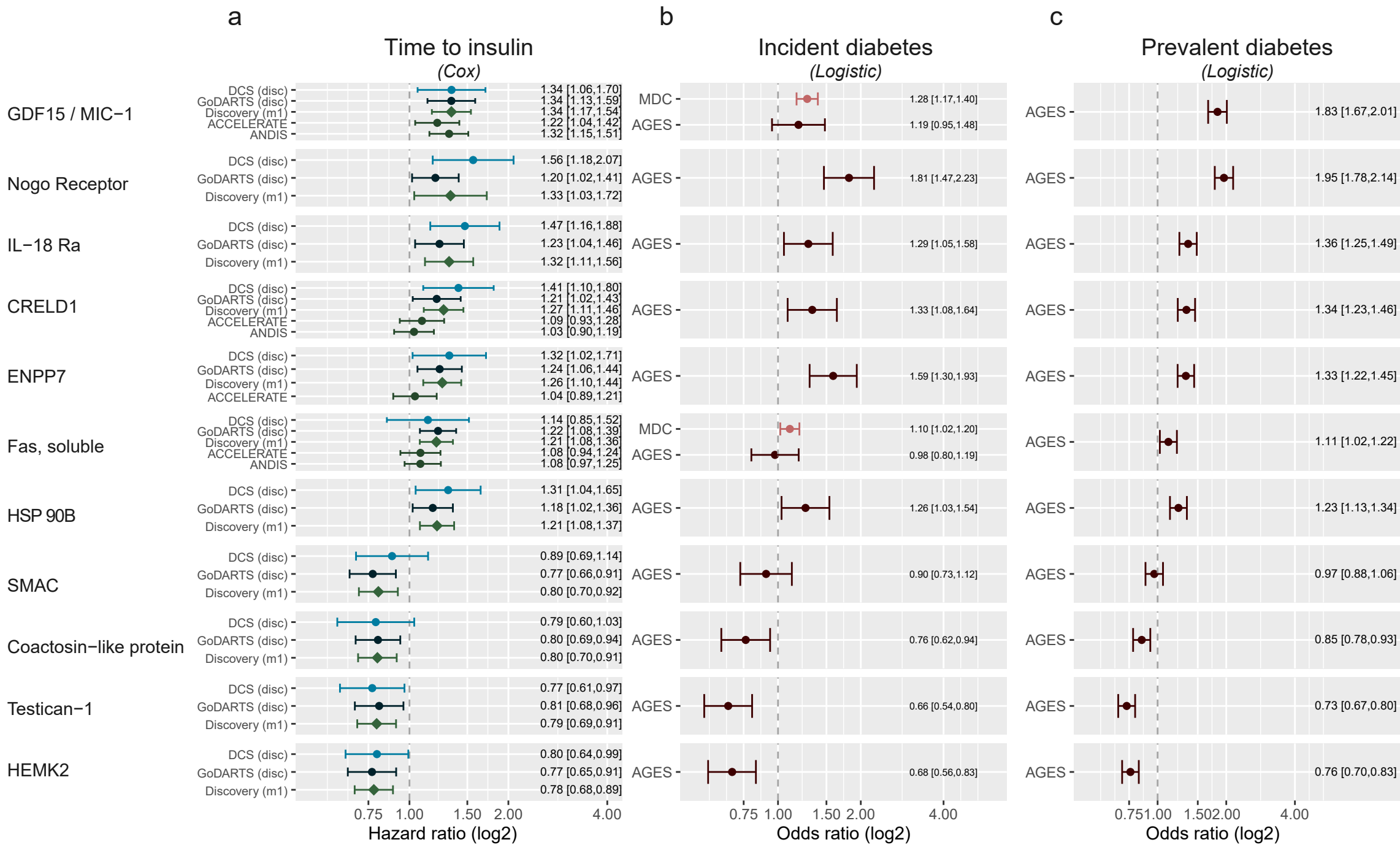


Fig. 3

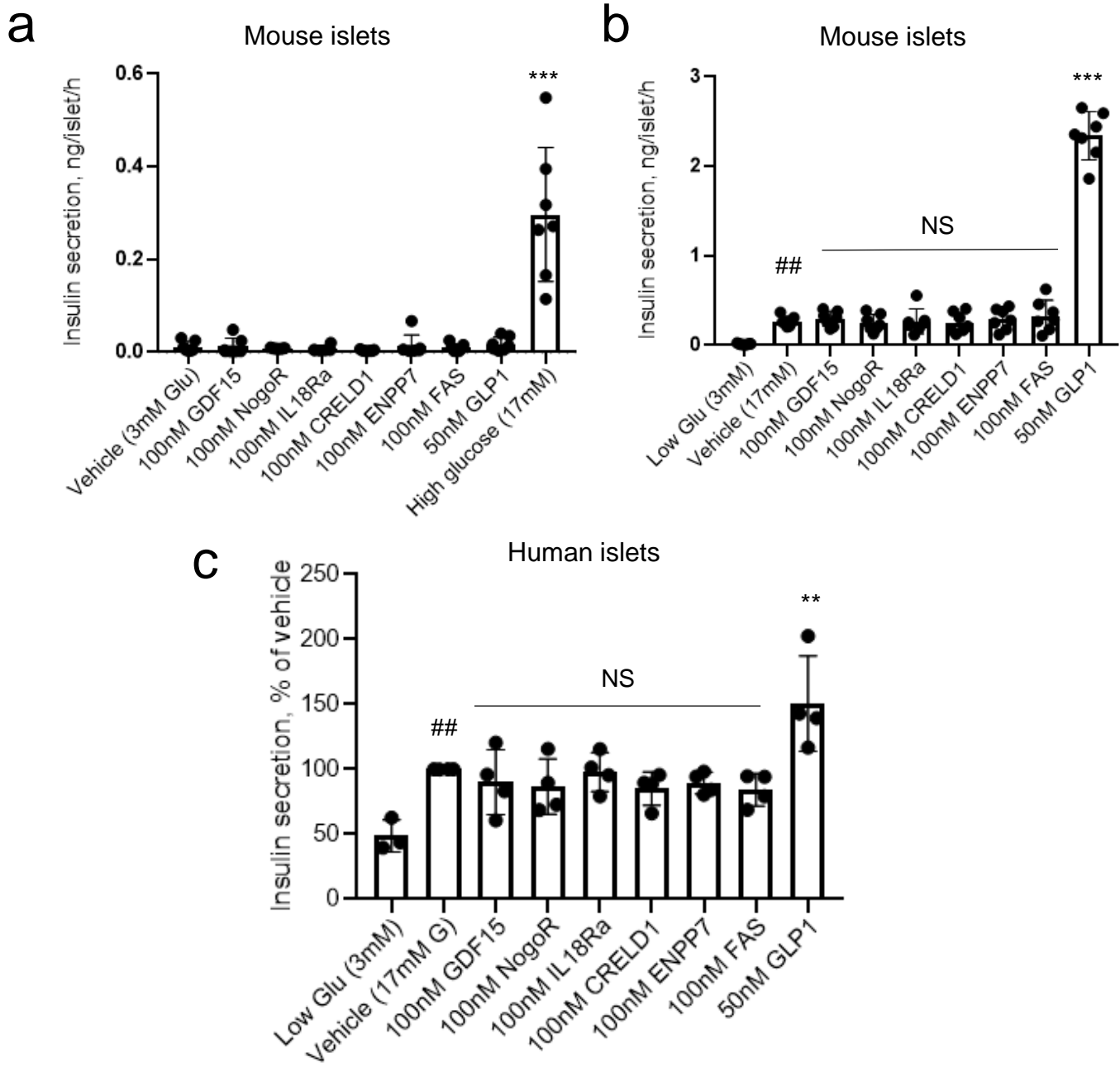


Fig. 4

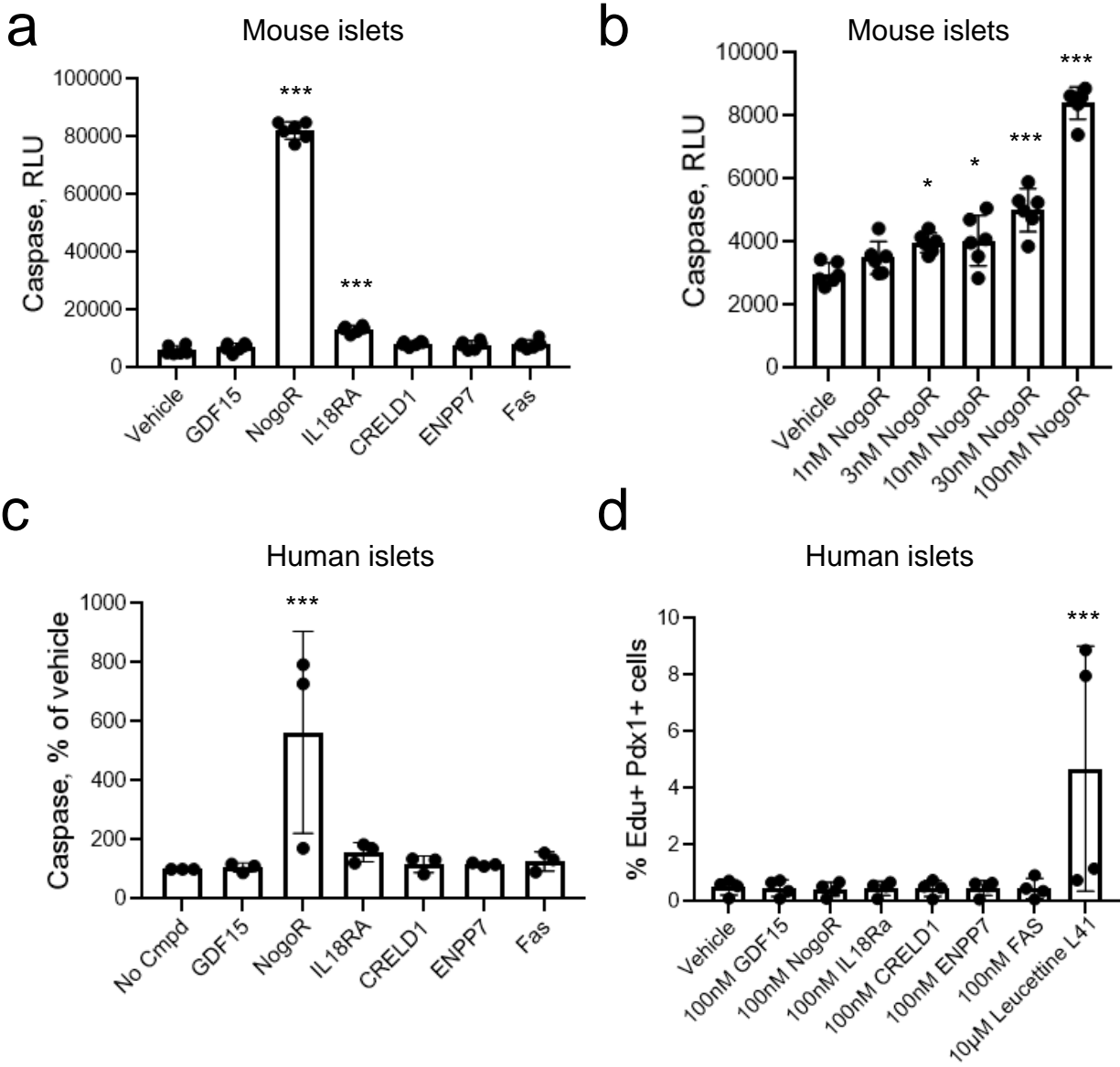


Fig. 5

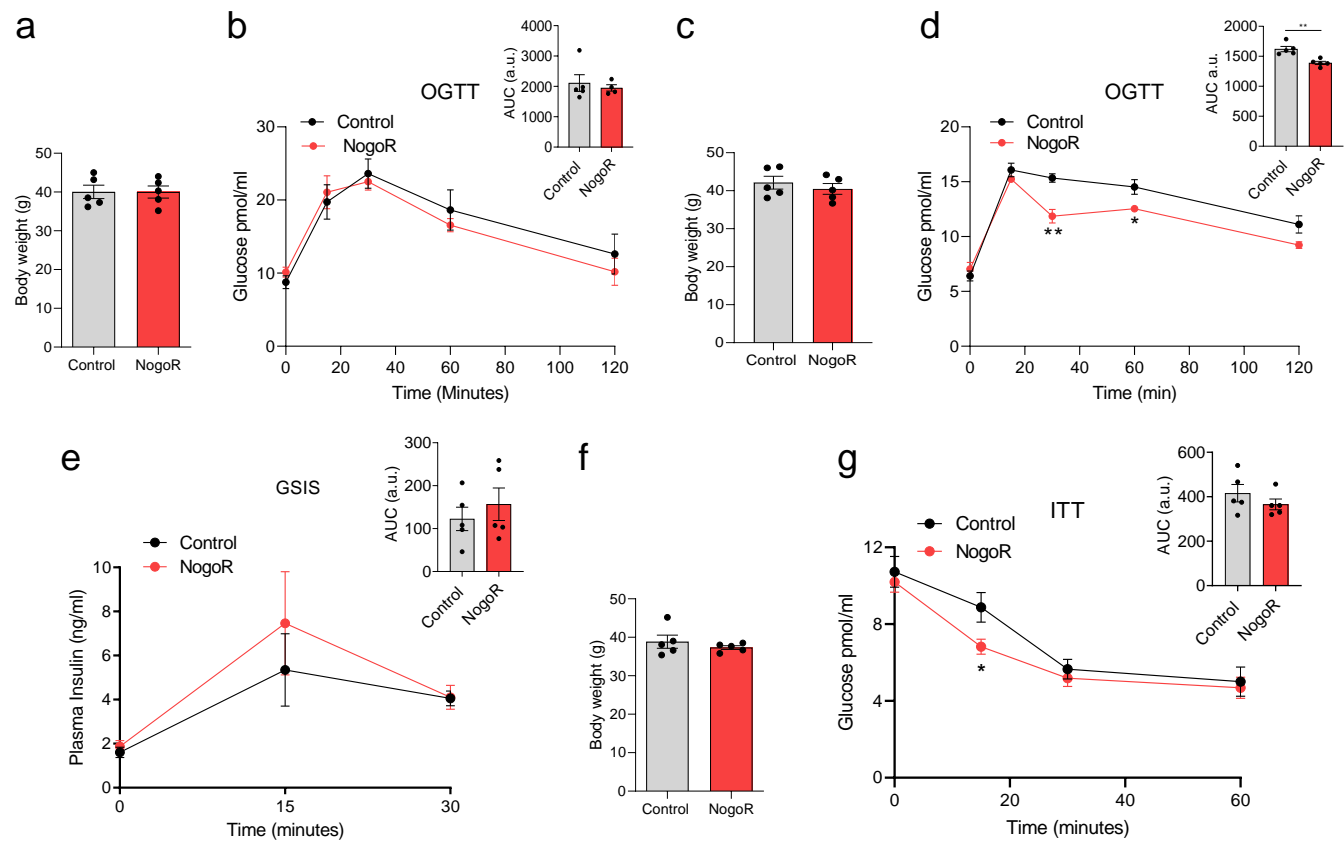
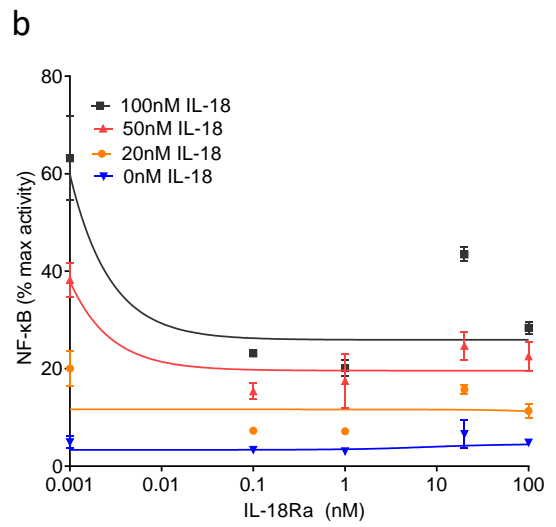
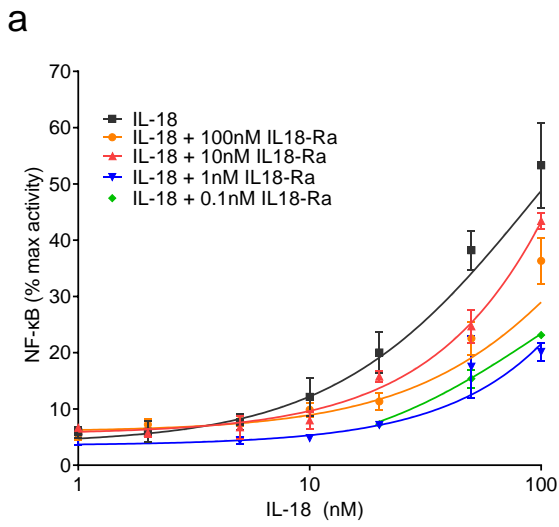


Fig. 6



| | 0nM IL18-Ra | 100nM IL18-Ra | 10nM IL18-Ra | 1nM IL18-Ra | 0.1nM IL18-Ra |
|----------|----------------|------------------|-----------------|----------------|------------------|
| EC50, nM | 93.78 | 300.9 | 925.2 | 794445 | 102.4 |
| logEC50 | 1.972 | 2.478 | 2.966 | 5.900 | 2.010 |

| | 100nM IL-18 | 50nM IL-18 | 20nM IL- 18 | 0nM IL-18 |
|----------|----------------|---------------|----------------|--------------|
| IC50, nM | 1.368 | 1.402 | 1.723 | 0.8448 |
| logIC50 | 0.1361 | 0.1467 | 0.2363 | -0.0732 |

Fig. 7